ORGANOMETALLICS

Article

Cite This: *Organometallics* XXXX, XXX, XXX−XXX

Comprehensive Experimental and Computational Study of η^6-Arene Ruthenium(II) and Osmium(II) Complexes Supported by Sulfur Analogues of the β-Diketiminate Ligand

Crystal O'Connor, Darren C. Lawlor, Conor Robinson, Helge Müller-Bunz, and Andrew D. Phillips*

School of Chemistry, University College Dublin, Belfield, Dublin 4, Ireland

Supporting Information

ABSTRACT: In comparison to β-diketiminates, a highly exploited class of *N*,*N*-chelating ligands, the corresponding β-thioketoiminates, monothio-substituted analogues, have received only minor attention. β-Thioketoiminates are straightforwardly prepared through treatment of an appropriate β-ketoiminate with Lawesson's reagent. Employing standard synthetic techniques for η^6-arene Ru(II) and Os(II) β-diketiminate complexes, an analogous series of chlorido-metal complexes supported by different sized *N*-aryl substituted β-thioketoiminate ligands is reported. However, metal ligation of a β-thioketoiminate bearing an electron-withdrawing CF_3 group was not possible. The metal−chlorine bond in these complexes is readily activated by various sodium or silver salts of weakly coordinating anions, affording coordinately unsaturated cationic formally 16-electron species. All η^6-C_6H_6 metal β-thioketoiminate complexes were characterized by NMR and in the solid state using single crystal X-ray diffraction techniques. Structural studies reveal that incorporation of a thio-group induces substantial bond angle distortion within the metallocycle. The reactivity of the cationic η^6-C_6H_6 Ru(II) β-thioketoiminate complexes toward alkynes and isonitriles is analogous to that of the β-diketiminate species. Specifically, the reaction with 1-hexyne results in a [4 + 2] cycloaddition involving the metal and β-C sites, while reaction with isonitrile completely displaces the η^6-C_6H_6 ligand. A comprehensive DFT study employing charge decomposition analysis (CDA) reveals a strong covalent metal−sulfur bond which dominates the metal β-thioketoiminate interaction. The M−S bond (M = Ru or Os) is strengthened by charge transfer from metal to sulfur, in contrast to the β-diketiminate species where back electron donation from the metal to the nitrogen centers is negligible. The first reported β-selenoketoiminate was prepared by reacting a β-ketoiminate with the Woolins' reagent. However, this seleno-analog demonstrated significant instability with respect to hydrolysis, and coordination to an η^6-arene Ru(II) or Os(II) moiety proved unsuccessful.

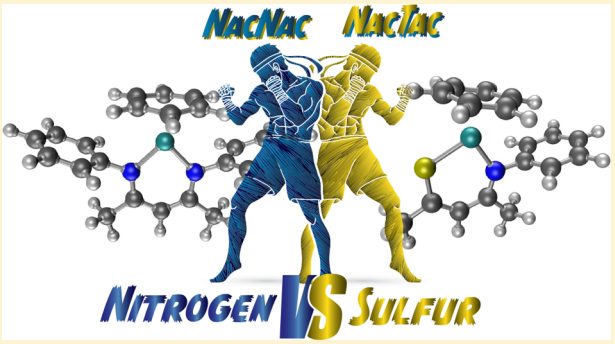

INTRODUCTION

The chelating anionic β-diketiminate class of ligand (NacNac) has engendered significant interest over recent years, affording a diverse range of novel transition metal complexes with unusual bonding properties and chemical reactivity.[1−7] Within the group 8 triad, the well-documented class of iron-centered β-diketiminate complexes has exhibited a range of chemical behavior with the ability to activate extremely inert bonds including those of N_2.[8,9] Moreover, the application of sterically bulky β-diketiminate ligands has enabled the isolation of complexes representing trapped catalytic intermediates which has been instrumental for the further elucidation of reaction mechanisms.[10] In recent years, complexes involving the heavier members of the group 8 triad, Ru and Os, have also been reported, Scheme 1. Phillips and Dyson et al. described a series of chlorido-substituted (**1a**,**b**) and cationic (**2a**−**d**) η^6-arene coordinated Ru(II)[11,12] and Os(II)[13] complexes supported by β-diketiminate ligands featuring strong donor and steric influence, imparted through alkyl *ortho*-substitution on the flanking *N*-aryl groups. Conversely, Ru β-diketiminate complexes with reduced donating capability imparted by the inclusion of fluoroalkyl substituents were also reported.[14,15] A prominent feature of cationic η^6-arene coordinated Ru(II) and Os(II) β-diketiminato complexes (**2a**,**b**) is the ability to undergo reversible bifunctional cycloaddition reactions with substrates containing π-unsaturated bonds (Scheme 1),[16,17] whereby alkynes form highly stable tripodal adducts. Similarly, molecular dihydrogen is readily activated to afford Ru(II)- or Os(II)-β-diimine hydrido complexes (Scheme 1).[12]

Complexes **2a** and **2b** demonstrate versatility as catalysts for a number of synthetic applications including the homogeneous dehydrogenation of amine boranes,[13,18] alkene hydrogenation,[11,12] and Diels−Alder cycloaddition reactions.[15]

Recently, O'Connor et al. have expanded this series of η^6-arene Ru(II) compounds to include the β-ketoiminate ligand featuring mixed N,O coordinating centers. Furthermore, we

Received: February 23, 2018

DOI: 10.1021/acs.organomet.8b00111
Organometallics XXXX, XXX, XXX−XXX

Scheme 1. Structure and Reactivity of Chlorido-Substituted (1a−b) and Cationic (2a−d) η^6-Arene-Ru(II) and -Os(II) β-Diketiminate Complexes

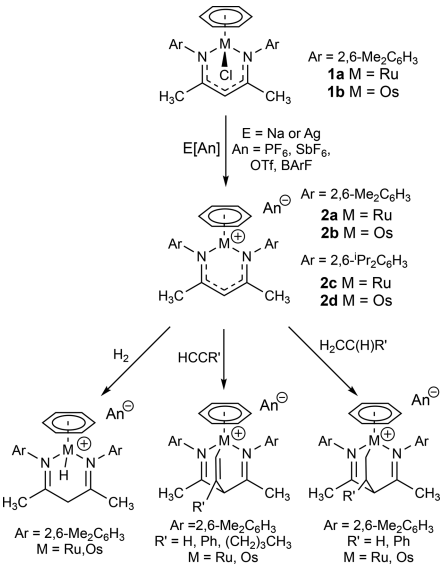

previously reported the first example of a Ru(II) complex supported by a *N*-aryl anilidoimine ligand.[18]

This report focuses on extending the range of complexes featuring π-unsaturated monoaza anionic ligands incorporating either a coordinating sulfur or selenium center (Scheme 2). In

Scheme 2. Structures of Nitrogen, Oxygen, and Sulfur π-Bonded Heterocyclic Protonated Ligand Precursors

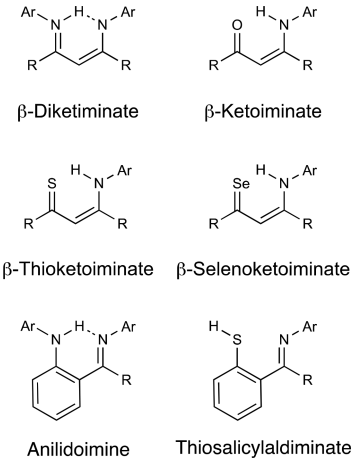

contrast, numerous Ru complexes featuring coordinately saturated thio-based ligands are known,[19−21] while ligands based on selenium[22,23] and tellurium[23,24] are significantly rarer. Singh et al. reported several half-sandwich Ru(II) complexes bearing tridentate ligands incorporating sulfur, selenium, and tellurium as the coordinating centers.[25] The corresponding complexes are efficient transfer hydrogenation catalysts for various types of ketones and are proposed to operate via a bifunctional mechanism. Moreover, these species are also oxidation catalysts for substituted alcohols. These complexes afforded conversion rates which are correlated with the strength of the metal−chalcogen bond. On the basis of this and other reports, we hypothesized that substituting the oxygen or nitrogen center of β-ketoiminate or β-diketiminate respectively with sulfur or selenium would modulate metal−ligand interactions and hence the reactivity of the resulting complexes.

In contrast to β-ketoiminates or β-diketiminates, the synthesis of β-thioimines or β-aminothiones are described through only a handful of literature references.[26] Standard methodology for the conversion of a carbonyl functional group into a thio- or seleno-carbonyl involves the use of sulfur and selenium transfer agents. Duguary et al. prepared the first β-thioketoiminates, albeit in low yields, through the reaction of β-ketoiminates with excess phosphorus pentasulfide (P_4S_{10}).[26] Subsequently, Walter et al. reported increased yields employing Lawesson's reagent (LR) (Scheme 3).,[27,28] Since the initial

Scheme 3. Commercially Available Sulfur- and Selenium-Based Phosphetane Transfer Agents Employed in This Study

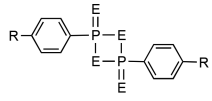

Lawesson's Reagent (LR) E = S, R = OCH_3
Woollin's Reagent (WR) E = Se, R =H

report of the putative *N*-phenyl β-thioketoiminate by Duguary, only a handful of variants have been prepared and characterized, including α-trifluoromethyl-α'-phenyl and α,α'-bis-phenyl substituted versions, but have not yet been employed as ligands.[30] In contrast, the synthesis of β-selenoimines (β-aminoselenones) are currently unreported; hence, this work details the first known preparation and characterization of this selenium version of a β-diketiminate ligand, employing the commercially available Woollins' reagent (WR) as the selenium transfer reagent (Scheme 3).[44−46]

A limited number of complexes featuring a β-thioimine are known, but include Cu(II),[31] Ti(IV),[32] Ni(II),[33] Pd(II), Pt(II),[34] Au(I),[35] and Cd(II),[36] where the metal center is bound by two coordinating thio-based ligands. The number of complexes bearing thiolated salicylaldimines is more extensive and examples containing first row metals from Fe to Zn, and several noble metals, i.e., Rh, Ir, Pt, and Pd are reported.[37−43] A few of these complexes have been used extensively as olefin polymerization catalysts.

RESULTS AND DISCUSSION

Synthesis and Characterization of β-Thio- and β-Seleno-ketoiminates. A series of β-thioketoiminates with different *N*-aryl substituents (**3a−d**) were synthesized from the corresponding β-ketoiminates employing LR in anhydrous 1,2-dimethoxymethane (Scheme 4). Previous reports indicated that the thionation process is generally complete within 1−2 h.[29] However, we found that optimum yields involved reaction times around 24 h. Moreover, it is observed that reaction times of >24 h have no discernible effect on the yield. The isolated β-

Scheme 4. Reaction Conditions Employed for the Synthesis of β-Thioketoiminates 3a−d

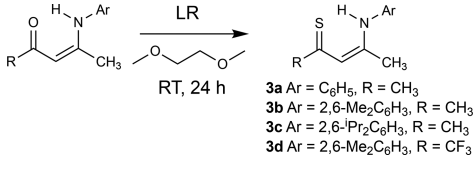

DOI: 10.1021/acs.organomet.8b00111
Organometallics XXXX, XXX, XXX−XXX

thioketoiminates are viscous red oils with yields of 70−90%, except for the least sterically encumbered compound **3a** at 17%.

The synthesis of two differently substituted *β*-selenoketoiminates (**4a**,**b**) were accomplished in an analogous manner with some key modifications (Scheme 5). Critical to the

Scheme 5. Reaction Conditions Employed for the Synthesis of *β*-Selenoketoiminates 4a,b

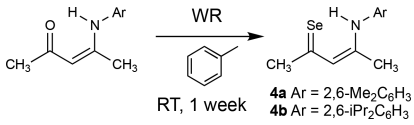

successful isolation of **4a**,**b** was the judicial selection of solvent, where various types of glymes, used in synthesis of **3a**−**d**, resulted in yields <10%. The highest yielding method consisted of combining the *β*-ketoiminate precursor with 0.5 equivalents of WR dissolved in anhydrous toluene.[46] After the first 24 h, ^{1}H NMR of the reaction mixture revealed a 50:50 mixture of *β*-selenoketoiminate and the precursor. Addition of another 0.5 equivalents of the WR reagent with reaction stirring for 1 week proved beneficial toward obtaining a moderate yield. The stability of **4a**,**b** differed significantly from that of the thiolated analogues. Compounds **4a**,**b** are viscous red oils; however, if kept in solution, a gradual color change from red to yellow is observed within 12 h, at which point ^{1}H NMR analysis revealed reformation of the precursor *β*-ketoiminate.

The ^{1}H NMR spectra of **3a**−**d** and **4a**,**b** are very distinctive in comparison to the precursory *β*-ketoiminates, particularly the δ(H) of N−H and *β*-H positions. Selected δ(^{1}H) and δ(^{13}C) values are provided in Table 1. For *β*-ketoiminates and *β*-diketiminates, δ(H) of *β*-H is between 5.0 and 5.5 ppm and δ(H) N−H is between 11 and 12 ppm.[47−49] In contrast, the *β*-thio- and *β*-seleno-ketoiminates are strongly deshielded with δ(H) *β*-H around 6.35−6.84 ppm, and δ(H) of N−H is extremely deshielded, i.e., 15.33−15.61 ppm. The similar electronegativity values of S and Se thus imparts greater *π*-type character to the core atoms of *β*-thio- or -seleno-ketoiminates. Therefore, δ(H) indicates that the *β*-H has electron density analogous to that of aromatic type protons. The δ(^{13}C) values for the C═S bonds are more deshielded compared to those of thiocarbonyl groups bonded to amides, i.e., PhC(S)NH$_2$, 202.1 ppm,[50] but considerably shielded as compared to those of alkyl-substituted thiocarbonyls (270−280 ppm).[51] The exception of the series is **3d** which has a deshielded signal for C═S due to the neighboring *α*-CF$_3$ group. Likewise, the δ(^{13}C) values of the C═Se bonds are within the range reported for other compounds featuring selenium carbonyls attached to amide groups (202−206 ppm).[52]

The solid-state structure of **3a** resolved by X-ray diffraction (Figure 1) reveals a *Z*-conformation typically associated with *N*-

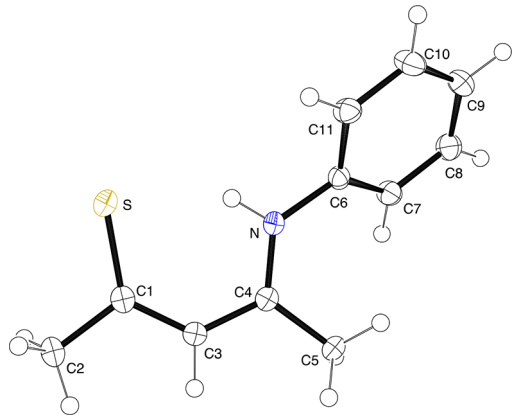

Figure 1. ORTEP representation of **3a**. Thermal ellipsoids are drawn with 50% probability. Selected bond distances (Å) and angles (deg): N−C4 1.332 (15); S−C1 1.694 (12); C4−C3−C1 128.57 (11); N−C4−C5 121.37 (10); S−C1−C2 116.64 (8).

aryl substituted *β*-enaminoketones. Compared to the *β*-diketiminate analogue of **3a**, the replacement of a *N*-phenyl group with S causes a distinctive distortion at the C(α)═S center as typified by a wide C4−C3−C1 bond angle, indicating a high degree of s-bonding character at the *β*-C site and supported by the extensive deshielding at this position as observed by ^{1}H NMR. As with *β*-diketiminates and *β*-ketoiminates, intramolecular hydrogen bonding is observed between the S and N centers, with the latter as the H donor, affording a distance of 2.960(1) Å. The N−C bond in **3a** (1.334(2) Å) is longer than the imine bond of 1.314 Å in the protonated *N*-phenyl *β*-diketiminate.

Synthesis of Chlorido-Substituted η^6-Arene Ru(II) and Os(II) *β*-Thioketoiminate Complexes. To facilitate complexation of the η^6-benzene Ru(II) or Os(II) moiety, *in situ* preparation of the corresponding lithiated *β*-thioketoiminate (**3a**−**c**) was performed and subsequently added to 0.5 equivalents of (M(η^6-C$_6$H$_6$)Cl$_2$)$_2$ dimer (M = Ru or Os). After 24 h, a standard workup procedure afforded complexes **5a**−**c** and **6** with yields of 44−89% (Scheme 6). Complexes **5c** and **6** featuring 2,6-^{i}Pr$_2$C$_6$H$_3$ as the *N*-aryl group are the most kinetically stable of the series and provided the highest yields. Moreover, both species are highly air and moisture stable both in the solid state and solution with no visible signs of decomposition as monitored by solution ^{1}H NMR over a period of several months. In contrast, the analogous Ru and Os *β*-diketiminate complexes degrade within several hours upon exposure to atmospheric conditions. Reducing the size of the *N*-aryl group resulted in dramatically decreased yields for the

Table 1. Selected ^{1}H and ^{13}C{^{1}H} Chemical Shift Data (ppm) for *β*-Thioketoiminates 3a−d and *β*-Selenoketoiminates 4a,b[a]

	3a	3b	3c	3d	4a	4b
			δ(^{1}H)			
β-H	6.26	6.45	6.35	6.84	6.71	6.66
N−H	15.56	15.33	15.30	15.46	15.60	15.61
			δ(^{13}C)			
β-CH	113.8	112.9	112.7	111.6	118.4	118.7
C═(S/Se)	207.6	205.9	206.9	184.0	204.3	204.3

[a]All spectra recorded in CDCl$_3$.

DOI: 10.1021/acs.organomet.8b00111
Organometallics XXXX, XXX, XXX−XXX

Scheme 6. Reaction Conditions Employed for the Synthesis of Chlorido-η^6-arene−Metal Complexes Supported by β-Thioketoiminate Ligands 5a−c (M = Ru(II)) or 6 (M = Os(II))

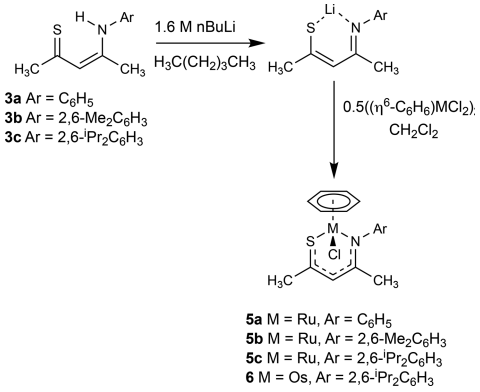

Ru complexes **5a,b** showing greater sensitivity to air and moisture, where **5b** decomposed within hours. Interestingly, the chloro-substituted η^6-C_6H_6 Ru complex featuring the highly bulky β-diketiminate ligand (2,6-^{i}Pr$_2$C$_6$H$_3$) cannot be synthetically prepared presumably due to strongly unfavorable steric interactions. The methodology for ligand complexation presented in Scheme 6 was not successful when applied in the case of **3d**. Alternatively, thallium alkoxides such as TlOEt which have been previously reported as highly effective deprotonation reagents and greatly facilitating the transmetalation process for numerous types of organo-ruthenium complexes and in particularly Ru complexes featuring perfluorinated β-diketiminate ligands[15] also proved ineffective, although a color change from red to dark brown is observed within 5 min upon reaction with TlOEt. Subsequently, the addition of $(Ru(\eta^6\text{-}C_6H_6)Cl_2)_2$ to this ligand failed to transmetalate, where ^{19}F NMR showed an abundance of uncomplexed ligand **3d** and several currently unidentified minor species.

Attempted Synthesis of an η^6-Arene Ru(II) β-Selenoketoiminate Complex. Coordination of the β-seleno-ketoiminate to an η^6-arene Ru(II) fragment was attempted with a variety of methodologies: First, through the standard *in situ* formation of a lithiated complex, followed by the transmetalation process. However, addition of the $(Ru(\eta^6\text{-}C_6H_6)Cl_2)_2$ dimer resulted in no apparent color change being observed, with almost all of the Ru dimer starting material recovered. Subsequent modifications to the reaction conditions revealed no formation of the target complex nor any starting material **4a** recovered as determined by ^{1}H NMR and ESI mass spectrometry. Instead, a series of overlapping manifold of peaks was observed, resembling spectra normally associated with polymeric substances; hence, it is likely the *n*-BuLi activates the β-seleno-ketoiminate beyond simple deprotonation. Two separate alternative methods of transmetalation were attempted with TlOEt and Ag_2O; the latter reagent proving valuable in some cases for coordinating highly fluorinated β-diketiminates to an η^6-arene Ru moiety.[13] However, both attempts were also unsuccessful. Hence, it is apparent that the *N*-aryl β-selenoketoiminate is too unstable in solution to survive the time required to complete transmetalation process.

Synthesis of Cationic η^6-Arene Ru(II) and Os(II) β-Thioketoiminato Complexes. Following the methodology developed for cationic η^6-arene Ru(II)- and Os(II)-β-diketiminate complexes **2a−d**,[12] chlorido substituents **5a−c** and **6** are readily abstracted using sodium or sliver salts featuring weakly coordinating anions, i.e., *tetrakis*-3,5-bis-(trifluoromethyl)phenyl borate (herein abbreviated as BArF) or PF_6 (Method A, Scheme 7). Moreover, formation of the triflate salts is a convenient one-pot procedure using a slight excess of [Na]OTf with lithiated **3b** or **3c** in the presence of the η^6-arene Ru chloride dimer (Scheme 7, Method B).[53] The resulting brown or dark green colored complexes are isolated in yields of 33−68%. Sensitivity of the cationic complexes to air and moisture was significantly more extreme than that of the chloride-substituted analogues, with exposure in the solid state or solution causing visible decomposition within minutes.

Scheme 7. Reaction Conditions Employed for the Synthesis of Cationic η^6-Arene Metal Complexes Supported by β-Thioketoiminates 7b,c (M = Ru(II)) or 8 (M = Os(II)) Using Method A or B *in Situ*

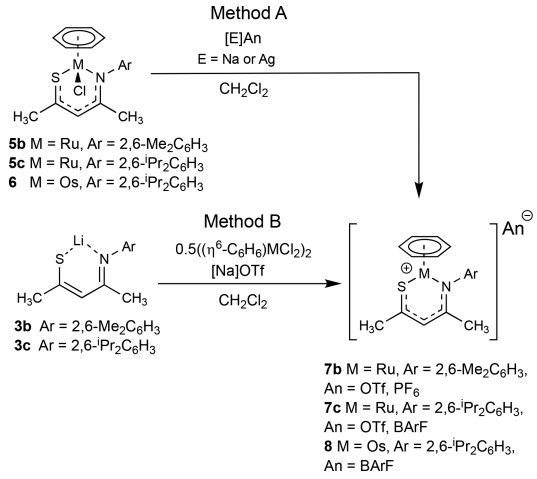

Structural Characterization in Solution. Diagnostic ^{1}H and ^{13}C{^{1}H} NMR signals of the chlorido-substituted and cationic β-thioketiminate organometallic complexes are given in Tables 2 and 3, respectively. Due to the π-conjugation within the chelating ligand, the $\delta(^1H)$ value of the β-H position provides important information regarding the relative electron density donated to the metal center. The β-H resonances for **5a−c** are shielded (5.75−5.88 ppm) compared to that of the protonated uncoordinated ligand. The apparent differences in steric profile associated with the *N*-aryl group have only a minor influence on the $\delta(^1H)$ β-H values. Os species **6** features the most deshielding β-H site. This trend is also paralleled for the protons associated with the η^6-arene, with **6** demonstrating the greatest deshielded signal, suggesting greater electron donation from this ligand to metal for Os compared to Ru. Analogous to the β-diketiminate complexes, cationic complexes **7b,c** and **8** present with significant deshielding of the $\delta(^1H)$ β-H site with values of 5.89−7.39 ppm. Thus, a strong indication of increased π-delocalization is associated with the core component of the coordinating β-thioketoiminate ligand. Moreover, the $\delta(^1H)$ associated with the η^6-benzene changes from 4.9 ppm with Cl-substitution to 6.22 ppm for **7b** and 7.39 ppm in **7c**; these values approach that of free benzene, i.e., 7.35 ppm (in CD_2Cl_2).[54] This suggests that the η^6-arene ligand is not as strongly donating as that in the Cl-coordinated compounds. The ^{1}H NMR data also suggests that there are negligible differences for the type of *N*-aryl employed, i.e., **7b**

DOI: 10.1021/acs.organomet.8b00111
Organometallics XXXX, XXX, XXX−XXX

Table 2. Selected ^{1}H and ^{13}C{^{1}H} Chemical Shift Data (ppm) for the η^6-C_6H_6 Ru(II) and Os(II) Complexes Bearing β-Thioketoiminate Ligand: Chlorido-Substituted Complexes 5a−c and 6 and Triflato-Substituted and Cationic Species 7b,c and 8[a]

	5a	5b	5c	6	7b (OTf)	7b (PF_6)	7c (OTf)	7c (BArF)	8 (BArF)
metal	Ru	Ru	Ru	Os	Ru	Ru	Ru	Ru	Os
					^{1}H				
η^6-C_6H_6	4.91	4.93	4.99	5.16	5.04	5.80	5.01	5.79	6.38
β-*CH*	5.75	5.88	5.85	6.03	6.06	6.22	5.89	7.39	7.83
					^{13}C{^{1}H}				
η^6-C_6H_6	87.0	86.8	86.5	78.2	87.1	84.7	85.0	85.0	78.9
β-CH	116.9	120.0	119.6	122.1	120.5	119.4	120.5	119.5	118.1
C═S	166.7	166.4	167.0	167.5	167.6	173.9	167.6	173.5	176.1
C═N					166.3	168.2	165.8	170.1	170.3

[a]All spectra recorded in CD_2Cl_2.

Table 3. Selected ^{1}H and ^{13}C{^{1}H} Chemical Shift Data (ppm) for Cationic η^6-C_6H_6 Ru(II) and Os(II) Complexes Supported by Either a β-Thioketoiminate (7c and 8) or a β-Diketiminate (2a,b) Ligand[a]

	7c (PF_6)	8 (BArF)	2a (OTf)	2b (OTf)
metal	Ru	Os	Ru	Os
		^{1}H		
η^6-C_6H_6	5.79	6.37	5.04	5.79
β-*CH*	7.39	7.82	6.06	7.00
		^{13}C{^{1}H}		
η^6-C_6H_6	85.0	78.1	84.1	77.1
β-CH	120.5	117.4	105.6	107.9
C═S	167.6	175.8		
C═N			163.9	165.7
ref	herein	herein	12	13

[a]All spectra recorded in CD_2Cl_2.

versus **7c**, as both di-*ortho*-alkyl substituted aryl groups are expected to have similar steric repulsive effects toward the η^6-arene metal fragment. A comparison between complexes bearing the triflato group against those with a weakly coordinating anion (PF_6 or BArF) shows more shielded resonances, especially for the β-H position, with values similar to those of the Cl-substituted complexes. Similarly, the δ(^{13}C) values of the β-C, C═N, and C═S positions reflect subtle but notable differences when triflato is employed. Thus, in contrast to Ru β-diketiminate complex **2a**, a weak Ru−O(SO_2CF_3) bond in solution exists in **7b** and **7c**. For cationic Os complex **8**, again the increased deshielding of the β-H and the η^6-arene protons is consistent with increased electron donation from the β-thioketoiminate, with the β-H site being the most deshielded of all the complexes described, while the η^6-arene gains more π-delocalized character, indicating a decreased π-back bonding with the metal center. Interestingly, there is a large increase in shielding of the C═S position in all cases, as the δ(^{13}C) values ~205 ppm change to 167 ppm in **7c** and **8**. However, as ^{13}C chemical shifts are influenced partially by paramagnetic contributions, changes in δ(^{13}C) values are not directly related to alterations in electron density of the S═C bond, but more by changes in the energy of the n $\rightarrow\pi^*$ transition.[55,56]

In comparison of δ(^{1}H) values for the β-H and η^6-arene protons associated with the cationic η^6-C_6H_6 Ru(II) and Os(II) β-diketiminate complexes (**2a**,**b**) with the analogous *N*-^{i}Pr$_2$$C_6H_3$ substituted **7c** and **8** (Table 3) suggest greater π-delocalization in the β-thioketoiminate cases, in parallel with weaker a bonding interaction between the η^6-arene and metal. Thus, the NMR data suggests a stronger metal−ligand interaction exists in the case of the β-thioketoiminate as compared to β-diketiminate. Moreover, this enhanced bonding diminishes the interaction between the metal and η^6-arene.

Solid-State Structural Characterization. Chlorido-complexes **5b**,**c** and **6** were characterized in the solid-state by X-ray diffraction analysis (**5c** shown in Figure 2, **5b** and **6** shown in Figures S2 and S3). A comparison of relevant metric parameters is given in Table 4. All complexes presented with a piano-stool type geometry typical of heavy group 8 metal complexes bearing an η^6-arene ligand. Previously, we reported that sterically bulky β-diketiminate Ru(II) and Os(II) complexes containing a M−Cl bond, exhibit a strong folding along a vector defined by the two coordinating nitrogen centers. This structural feature is also present for the herein described β-thioketoiminate complexes where the fold occurs along the N,S-vector (Figure 5). A second less prominent fold also occurs through the N,S-chelating ligand along a vector defined by metal and β-C position. The solid-state packing of chloro-substituted complexes **5b**,**c** and **6** are characterized by short intermolecular contacts between the S center and a hydrogen associated with an η^6-arene, as detailed in the Supporting Information. Complexes **5b** and **5c** possess long Ru−Cl bond distances of 2.437(5) and 2.432(3) Å,

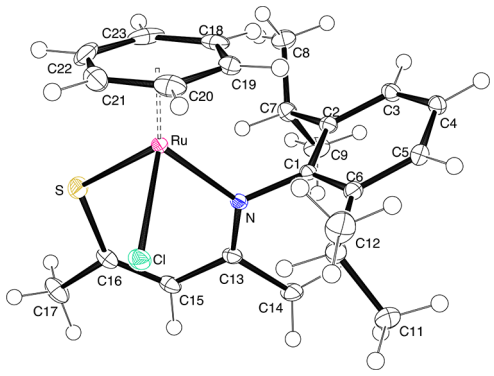

Figure 2. ORTEP representation of **5c**. Thermal ellipsoids are drawn with 50% probability. Selected bond distances (Å) and angles (deg): Ru−Cl 2.432(3); Ru−C(cent) 1.693 (6); Ru−N 2.133 (1); Ru−S 2.338 (4); S−C(16) 1.703(2); N−C(13) 1.309(2); S−Ru−N 90.49(3); C(16)−C(15)−C(13) 129.72(1); C(cent)−Ru−N/S-(midpoint) 150.47(3); Ru−N/S(midpoint)−C(15) 153.45(5), Ru−N−C(1) 113.27(8); Ru−N−C(13) 128.89(9); Ru−S−C(16) 110.95(5).

DOI: 10.1021/acs.organomet.8b00111
Organometallics XXXX, XXX, XXX−XXX

Table 4. Selected Crystallographic Data for Chlorido-Substituted η^6-C_6H_6 Ru(II) and Os(II) Complexes Bearing a β-Thioketoiminate or β-Diketiminate Ligand[a]

parameter[b]	5b	5c	6	1a	1b
metal (M)	Ru	Ru	Os	Ru	Os
M−N	2.142(1)	2.133(1)	2.132(1)	2.099(2)	2.123(4), 2.127(4)
M−S	2.332(1)	2.338(1)	2.344(1)		
M−Cl	2.437(1)	2.432(1)	2.443(1)	2.521(1)	2.416(1)
M−C(cent)	1.689(1)	1.693(1)	1.685(1)	1.688(1)	1.693(3)
N=C(α)	1.303(3)	1.310(2)	1.314(2)	1.335(3)	1.296(6), 1.280(7)
S=C(α)	1.709(2)	1.703(2)	1.706(2)		
C(N)−C(β)	1.442(3)	1.442(2)	1.438(2)	1.394(3)	1.500(8), 1.486(8)
C(S)−C(β)	1.351(3)	1.361(2)	1.364(2)		
N−M−S	87.8(1)	90.5(1)	90.7(1)		
N−M−N				86.6(1)	84.7(2)
M−N−C(*ipso*)	112.0(1)	113.3(1)	113.6(1)	118.5(2)	116.9(3), 115.5(3)
M−N−C(α)	130.2(1)	128.9(1)	128.8(1)	124.7(2)	126.3(4), 121.8(5)
M−S−C(α)	109.8(1)	111.0(1)	111.4(1)		
N−C(α)−C(β)	125.3(2)	126.0(1)	126.5(1)	124.4(3)	121.6(5), 122.8(5)
S−C(α)−C(β)	126.8(2)	126.9(1)	126.5(1)		
C(α)−C(β)−C(α)	127.9(2)	129.7(1)	130.1(2)	126.5(1)	118.9(4)
C(cent)−M−Cl	125.5(1)	124.4(1)	125.2(1)	122.2(1)	123.7(1)
C(cent)−M−N/S(midpoint) (ϕ)	148.0(1)	150.4(1)	151.4(1)		
C(cent)−M−N/N(midpoint) (ϕ)				154.1(1)	152.6(1)
M−N/S(midpoint)−C (θ)	147.9(1)	153.5(1)	154.7(1)		
M−N/N(midpoint)−C (θ)				154.8(2)	145.0(2)
ref	herein	herein	herein	12	13

[a]Bond lengths in Å and angles in degrees. For the definition of the folding angles ϕ and θ, see Figure 4. [b]C(cent): refers to centroid point of the η^6-C_6H_6 ligand.

respectively. These values are longer than the median value of 2.38 Å for all η^6-arene type complexes with a Ru−Cl bond as indicated by the Cambridge Structural Database (CSD),[57] but are significantly shorter than M−Cl 2.526(2) Å in **1a**.[12] Interestingly, Os complex **6** has a M−Cl bond distance of 2.443(1) Å, and in this case, longer than that in β-diketiminate counterpart **1b**, 2.416(1) Å.[13] As expected for species **5b** and **5c**, the longer S=C(α) and Ru−S have an effect of widening the C(α)−C(β)−C(α) bond angle. While the Ru−S bond is equivalent between **5b** and **5c**, the Ru−N bond changes with different types of N-aryl substituents, whereas a shorter Ru−N bond in **5c** is observed when the N-aryl group is a bulkier 2,6-diisopropylphenyl. This change is also reflected in a longer N=C(α) bond and a wider N−Ru−S bond angle for **5c**. A search of the CSD shows a median Ru−S bond distance of 2.403 and 1.706 Å for a S−C and S=C bond, respectively.[57] Hence, **5b** and **5c** both feature Ru−S bond distances which are typically associated with S=C bonds. Complex **6** processes a longer M−S bond, but the S−C distance is equivalent to the Ru analog. In contrast, the imine bond is only slightly shorter. The S−Ru−N bite angles of 87.7(1)° for **5b** and 90.5(1)° in **5c** are comparable to the N−Ru−N bite angle of 86.7(1)° in **1a**. A characteristic feature of all herein described β-thioketoiminate complexes are the narrower M−S−C(α) bond angles which are roughly 18° less than the interior Ru−N−C(α) bond angles. The M−N−C(ipso) bond angles are less than those of the analogous β-diketiminate complexes. However, the internal ligand folding angles (θ, M−N/S−C(β)) are 147.9 and 150.4° for **5b** and **5c** which indicates that the core component of the ligand is not planar. Thus, analogous to β-diketiminate complexes, complex **5b**,**c** and **6** do not achieve complete π-delocalization within the core component of the β-thioketoiminate ligand; hence, an allylic π-type S−M−N interaction is expected as the primary interaction between the metal and S,N coordinating centers.

Cationic complexes **7c** and **8** were also characterized in the solid state (**7c** in Figure 3, **8** in Figure S4). For comparative purposes, corresponding cationic Ru and Os β-diketiminate complexes **2c**,**d**, bearing the highly bulky 2,6-diisopropylphenyl group as the flanking *N*-aryl, were prepared according to literature procedures and the solid state structures determined; see the Supporting Information. Selected metric parameters for all cationic Ru and Os complexes are given in Table 5. Removal

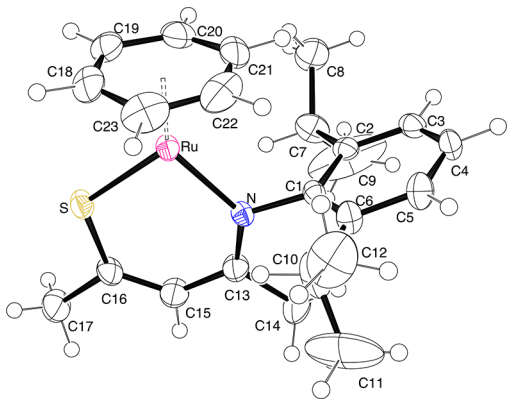

Figure 3. ORTEP representation of **7c** (BArF counterion). Thermal ellipsoids are drawn with 50% probability. The anion is omitted for clarity. Selected bond distances (Å) and angles (deg): Ru−C(cent) 1.692 (1); Ru−N 2.035 (2); Ru−S 2.214 (6); S−C(16) 1.696 (3); N−C(13) 1.329 (3); S−Ru−N 94.15 (1); C(16)−C(15)−C(13) 131.0 (2); C(cent)−Ru−N/S(midpoint) 172.33 (6); Ru−N/S(midpoint)−C(15) 168.9 (1); Ru−N−C(1) 113.55 (14), Ru−N−C(13) 130.33 (17); Ru−S−C(16) 113.88 (9).

DOI: 10.1021/acs.organomet.8b00111
Organometallics XXXX, XXX, XXX−XXX

Table 5. Selected Crystallographic Data for the η^6-C_6H_6 Ru(II) and Os(II) Complexes Bearing a β-Thioketoiminate Ligand[a]

parameter[b]	7c	8	2c[c]		2d
metal (M)	Ru	Os	Ru		Os
M−N	2.035(2)	2.025(2)	2.022(4) 2.021(4)	2.020(4) 2.022(4)	2.009(2) 2.012(2)
M−S	2.214(1)	2.227(1)			
M−C(cent)	1.692(1)	1.702(1)	1.710(2)	1.705(2)	1.701(1)
N═C(α)	1.329(3)	1.340(2)	1.351(6) 1.347(6)	1.354(6) 1.352(6)	1.347(2) 1.350(2)
S═C(α)	1.696(3)	1.702(2)			
C(N)−C(β)	1.419(4)	1.415(2)	1.402(8) 1.390(8)	1.392(8) 1.389(8)	1.385(3) 1.388(3)
C(S)−C(β)	1.359(4)	1.369(3)			
N−M−S	94.2(1)	94.1(1)			
N−M−N			89.8(2)	90.0(2)	89.7(1)
M−N−C(*ipso*)	113.6(1)	113.6(1)	116.3(3) 116.0(3)	117.3(3) 116.4(3)	116.8(1) 116.4(1)
M−N−C(α)	130.3(2)	130.6(1)	127.9(3) 127.7(3)	127.5(3) 127.5(3)	127.5(1) 128.0(1)
M−S−C(α)	113.9(1)	113.7(1)			
N−C(α)−C(β)	125.5(2)	125.9(2)	122.6(5) 123.1(5)	123.0(5) 123.1(5)	123.6(2) 123.0(2)
S−C(α)−C(β)	125.0(2)	125.2(1)			
C(α)−C(β)−C(α)	131.0(2)	130.5(2)	128.6(4)	128.7(4)	128.1(2)
C(cent)−M−N/S(midpoint) (ϕ)	172.3(1)	171.7(1)			
C(cent)−M−N/N(midpoint) (ϕ)			179.9(2)	178.3(1)	179.3(1)
M−N/S(midpoint)−C (θ)	168.9(1)	168.1(1)			
M−N/N(midpoint)−C (θ)			175.6(3)	180.0(4)	177.2(1)

[a]Bond lengths in Å and angles in degrees. Cationic species **7c** and **8**. For comparison, cationic complexes η^6-C_6H_6 Ru(II) β-diketiminate complexes **2c−d**. For the definition of the folding angles ϕ and θ see Figure 4. [b]C(cent): refers to centroid point of the η^6-C_6H_6 ligand. [c]Two crystallographically independent molecules are contained within the unit cell.

of the chlorido substituent from **5c** and **6**, induces a number of notable structural changes, including a significantly shortening of the M−N and M−S bonds by approximately 0.1 Å accompanied by a widening of the S−M−N bite angle. The metal to centroid distance of the η^6-arene is practically unchanged for the cationic Ru complex but increases for the Os species **8**. Interestingly, the N═C(α) bond lengthens in **7c** and **8** as compared to **5c** and **6**, whereas the S═C(α) bond remains invariant when the Cl group is removed and seemingly has only a slight effect on the M−S−C(α), M−N−C(α), and C(α)−C(β)−C(α) bond angles. The most dramatic changes between the Cl-substituted and cationic complexes is the flattening of the core component of the β-thioketoiminate ligand as indicated by the bond angle defined by the metal center, midpoint of the N,S atoms and the β-C (θ angle, Figure 4) which increases by nearly 15°. This modification enhances the overall π-delocalization throughout the chelating ligand. An additional striking feature is an approximately 20° increase in the ϕ angle (Figure 4) which relates the tilt of the η^6-arene with respect to the metal center and the β-thioketoiminate ligand. In comparison to the cationic β-diketiminate species, notable differences are the longer M−N bond lengths in the β-thioketoiminate species, which are matched by shorter N═C(α) bonds, particularly in the case of Ru. A comparison with β-diketiminate species **2c** and **2d** bearing the bulky 2,6-diisopropyl-phenyl groups shows a marked widening of the M−N−C(ipso) bond angles as compared to those in the β-thioketoiminate species, but only minor differences are observed in the interior N−C(α)−C(β) and the C(α)−C(β)−C(α) bond angles between the two different classes of

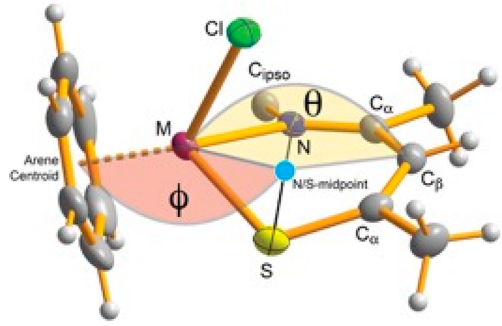

Figure 4. Atom labeling and definition of the folding angles (ϕ and θ) within the β-thioketoiminate supported complexes as defined by the centroid of the η^6-arene, the metal center, the midpoint between the N and S atoms, and the β-C site.

complexes. Interestingly, the intermolecular hydrogen bonding that exists with the S center of the β-diketiminate ligand in Cl-substituted species **5b,c** and **6** is not present in cationic species **7b** or **8**, and no intermolecular interactions with the S center are observed, suggesting that the increased bonding interaction with the metal centers reduces lone pair character on the coordinating S.

Chemical Reactivity of the η^6-Arene Ru(II) β-Thioketoiminato Complexes. Since the initial reports of η^6-arene Ru(II) β-diketiminate complexes, we have shown that the reactivity of these classes of compounds is strikingly different from that observed for other types of η^6-arene Ru(II) complexes including ones featuring β-diketonates,[58] which are

DOI: 10.1021/acs.organomet.8b00111
Organometallics XXXX, XXX, XXX−XXX

Scheme 8. Comparison of Reactivity between η^6-Arene-Ru(II) β-Diketiminate 2a and β-Thioketoiminate Complex 7b

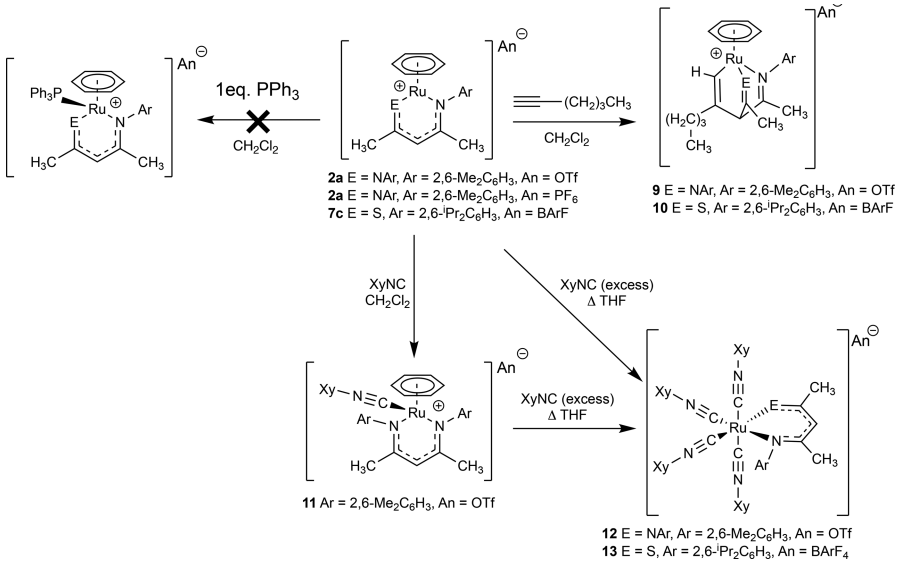

known to form simple coordination adducts with typical nucleophiles such as amines or phosphines (Scheme 8). The cationic 16-electron complexes **2a**,**b** exhibit bifunctional activity with a strong preference for undergoing [4 + 2] cycloadditions with alkenes and alkynes, in addition to reversible heterolytic activation of H_2.[12] As an initial probe into the reactivity of the cationic Ru(II) β-thioketoiminate complexes, the addition of PPh_3 to **7c** failed to demonstrate any adduction formation as monitored by ^{31}P NMR.[18] Similarly, triphenylphosphine does not bind to either **2a** or **2b**.

As demonstrated previously with acetylene, the reaction between 1-hexyne and Ru β-diketiminate species **2a** afforded **9** in quantitative yield. The analogous experiment was performed by first dissolving **7c** in CH_2Cl_2 and adding an excess of pure 1-hexyne. Instantly, a yellow color developed and with a standard workup, complex **10** was afforded with a yield of 86%. Recognition of adduct formation, i.e., **9** and **10**, is observed by both ESI-MS and ^1H NMR where the diagnostic singlet for the terminal "yne" proton occurs at $\delta(^1H)$ 9.22 ppm for **10** and 9.67 ppm for **9**. The extremely deshielded signal is caused by the orientation of this proton intersecting the deshielding cone of the η^6-arene ligand.[12,13]

Although phosphines do not form adducts with **2a**, neutral ligands with moderate σ-donor strength, and are also π-acceptors do interact with the Ru center and form coordination complexes as demonstrated by reacting **2a** with 1 equivalent of 2,6-dimethyl-isonitrile (herein abbreviated as XyNC). The resulting complex, **11**, was obtained as a red colored solid in high yield. Observation of the parent mass by ESI-MS confirmed **11** was a monocoordination adduct. The $\delta(^1H)$ of the diagnostic β-H position in **11**, 4.94 ppm, is almost identical to that of the chlorido-substituted complex **1a** and indicates a weakened interaction between the chelating ligand and metal center. A structure determined from X-ray diffraction studies displays the typical piano type geometry (Figure S13), where the β-diketiminate ligand presents with the standard folding pattern observed when an additional ligand is added to the Ru center.

The Ru−N bond lengths (2.098(2) and 2.095(2) Å) and N−Ru−N bond angle of 87.3(1)° are undistinctive. The Ru−C(N) bond length of 1.966(2) Å and the Ru−N−C 174.5(2)° bond angle are typical values and are comparable to those of other η^6-arene Ru complexes coordinated by a XyNC ligand.[59,61] The vibrational stretch of the C═N bond associated with Ru coordinated XyNC occurs at 2153 cm^{-1} and is shifted 33 cm^{-1} compared to that in the uncomplexed form, i.e., 2119.93 cm^{-1}. The modest change in frequency suggesting a minimal amount of π-back-donation. Alternating the reaction conditions, i.e., employing excess amount of XyNC and refluxing in dry THF for 24 h, afforded a bright purple solid **12**, in 79% yield.

Solution ESI-MS of complex **12** revealed that the parent molecular mass matches that of a Ru β-diketiminate fragment with four XyNC ligands. Morover, ^1H and $^{13}C\{^1H\}$ NMR confirmed loss of the η^6-C_6H_6 resonance and the $\delta(^1H)$ of the β-H position became shielded at 5.01 ppm. Other researchers have previously documented η^6-arene displacement from Ru by XyNC, particularly when the arene is *p*-cymene.[60] A structure of **12** resolved by X-ray crystallography studies reveals an octahedral Ru coordination environment with two equatorial XyNC ligands bonded *trans* to the chelating β-diketiminate ligand and the remaining two XyNC ligands occupying the axial positions. The two *trans*-positioned isonitriles feature shortened Ru−C bond distances as compared to those of the axial ligands. Although not reflected in the individual N−C(Xy) bond lengths, the solid-state IR of **12** shows three absorptions with frequencies of 2113, 2130, and 2190 cm^{-1} corresponding to four υ(NC) stretches. These values suggest considerable π-back bonding from the metal to π^* MOs of the XyNC ligands.[61] Of additional note is the significant folding present in the β-diketiminate ligand, 146.45(10)° which is greater than that observed for any η^6-arene or η^5-Cp* coordinated Ru β-diketiminate species.

Reaction between the cationic Ru β-thioketoiminate complex **7c** and 1 equivalent of XyNC resulted in a mixture of products. However, when an excess of isonitrile was employed with refluxing in anhydrous THF, a brown-yellow colored solid **13**, is obtained upon standard workup. Solution ESI-MS confirmed that the isotopic pattern of the parent peak matches that of a Ru β-thioketoiminate fragment with four coordinating XyNC ligands, **13**. In contrast to **12**, β-thioketoiminate species **13** features a highly deshielded β-H position, δ(H) = 6.25 ppm.

DOI: 10.1021/acs.organomet.8b00111
Organometallics XXXX, XXX, XXX−XXX

Solid-state IR of **13** reveals a strong unresolved absorption at 2083 cm^{-1}, which indicates that the π-back bonding between the Ru center and π^* MOs of the XyNC ligands is not as strong as those in the β-diketiminate complex **12**.

Although the η^6-arene Ru β-thioketoiminate complexes formally feature a single lone pair on the coordinating sulfur center, preliminary attempts to form simple coordination adducts using Lewis acids such as BF_3 or $Au(PPh_3)$ with **7c** were unsuccessful. For example, Goh et al. showed that one of the sulfur centers in the η^6-arene Ru thiapentane-1,5-dithiolate compound readily form an adduct with $Au(PPh_3)$.[62] For **7c**, it is unclear if steric hindrance prevented adduct formation or simply that the S lone pair is strongly deactivated in the cationic Ru β-thioketoiminate complexes.

Computational Study. The *in silico* studies reported herein were performed using the Gaussian 09 program[63] employing the hybrid GGA density functional ωB97XD that accounts for long-range dispersion effects.[64] As experimental structural parameters were obtained for both types of cationic Ru- and Os- β-diketiminate and β-thioketoiminate complexes containing the flanking 2,6-diisopropylphenyl as the *N*-aryl substituent, the computational study was limited only to the cationic formally 16-electron species (**I**–**IV**, Figure 6). All structures

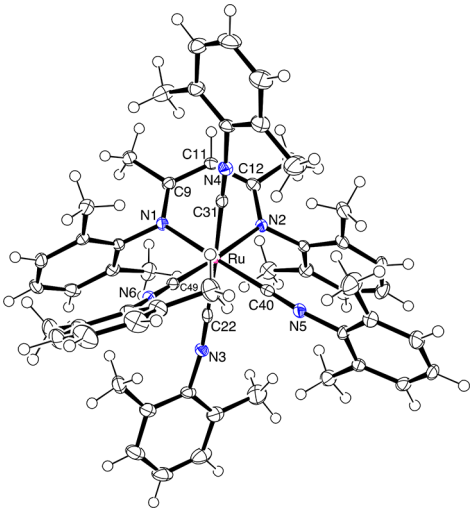

Figure 5. ORTEP representation of **12** (OTf). Thermal ellipsoids are drawn with 50% probability. The anion is omitted for clarity and only the core atoms of the ligands are indicated. Selected bond distances (Å) and angles (deg): Ru–C(22) 2.002 (3); Ru–C(49) 1.951 (3); Ru–C(40) 1.959 (3); Ru–C(31) 2.011 (3); Ru–N(1) 2.143 (2); Ru–N(2) 2.139 (2); C(22)–N(3) 1.161 (4); C(49)–N(6) 1.160 (3); C(40)–N(5) 1.164 (3); C(31)–N(4) 1.163 (4); N(1)–C(9) 1.325 (3); N(2)–C(12) 1.323 (4); N(1)–Ru–N(2) 86.60 (8); C(9)–C(11)–C(12) 127.6 (2); C(22)–Ru–C(31) 176.41 (10); C(40)–Ru–N(1) 176.97 (10); C(49)–Ru–N(2) 173.75 (10); Ru–N/N(midpoint)–C(11) 146.45 (10).

were geometrically optimized to an energy minimum and displayed structural metrics which are in excellent agreement with the experimental X-ray diffraction data. In particular, bond lengths and angles of the core metal–ligand components were satisfactorily reproduced with the M–N–C(ipso) bond angle parameters showing the greatest deviation up to 2°. Overall, the calculated bond lengths were 0.3–0.6% longer and the bond angles deviated from 0.5 to 2.6%. All calculated geometry parameters are well within acceptable standards for DFT modeling.[65] See the Supporting Information for a complete

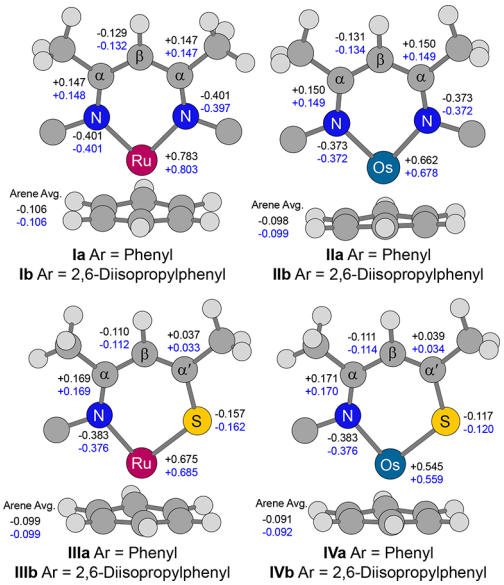

Figure 6. Comparison of atomic charges for cationic η^6-arene Ru- and Os-supported β-diketiminate and β-thioketoiminate complexes using the charge fitting scheme CM5. Values in black are complexes with *N*-phenyl substitution, and values in blue are complexes bearing *N*-2,6-diisopropylphenyl.

comparison of the experimental versus DFT calculated geometry.

As an initial means of comparison between the two classes of ligand, charge distribution through the complexes were determined using two of the more common methods for calculating atomic charge, the class II Hirshfeld analysis[66] and the class IV charge fitting method CM5, developed by Truhlar and Cramer (Table S5).[67] A typical alternating pattern of positively and negatively charged atomic centers is observed within the metallocyclic cores of the complexes **Ia**–**IVa** (Figure 6), where the β-C and N/S centers are negatively charged, while the metal and α-carbon sites are positive. In the case of β-diketiminate complexes **Ia**, the Ru center is more positively charged than Os (**IIa**), while the charges on the chelating ligands are relatively consistent except for the N centers. As expected, the overall charge distribution for β-thioketoiminate complexes **IIIa** and **IVa** are very different compared to those of **Ia** and **IIa**, where the metal center is less positively charged, while simultaneously the β-C position is less negatively charged. The incorporation of the less electronegative S center thus increases electron density on the metal and the adjoining α-C(S) site. Interestingly, the population analysis indicates increased charge on Os in **IVab**, while the S atom is more depleted than in the Ru case, **IIIab**. This suggests a greater interaction between Os–S. In comparison to Ru β-diketiminate species **Iab**, the single N center in β-thioketoiminate **IIIab** is more electronically depleted, while for both Os complexes, the charge on N is relatively similar.

Comparison of *N*-phenyl versus the significantly bulkier *N*-2,6-^{i}Pr$_2$C$_6$H$_3$ (herein abbreviated as dipp) substituent for both types of complex has the greatest effect on the metal center in terms of reducing electron density. To further quantify the electronic differences in metal interaction between the β-diketiminate and β-thioketoiminate ligands, a comparison of the Mayer bond indices (MBI) was performed for all bonds related to the metal center (Figure 7). MBIs provide a normalized index of bond strength, enabling a comparison

DOI: 10.1021/acs.organomet.8b00111
Organometallics XXXX, XXX, XXX–XXX

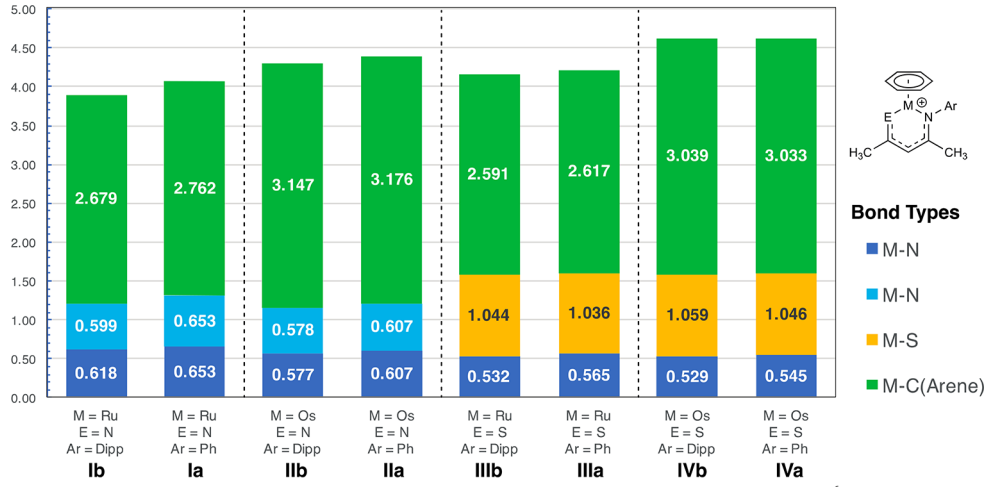

Figure 7. Mayer bond index comparison for all bonds involving the metal center for the cationic η^6-arene Ru- and Os-β-diketiminate (**I**, **II**) and β-thioketoiminate (**III**, **IV**) complexes with phenyl and dipp flanking *N*-aryl groups.

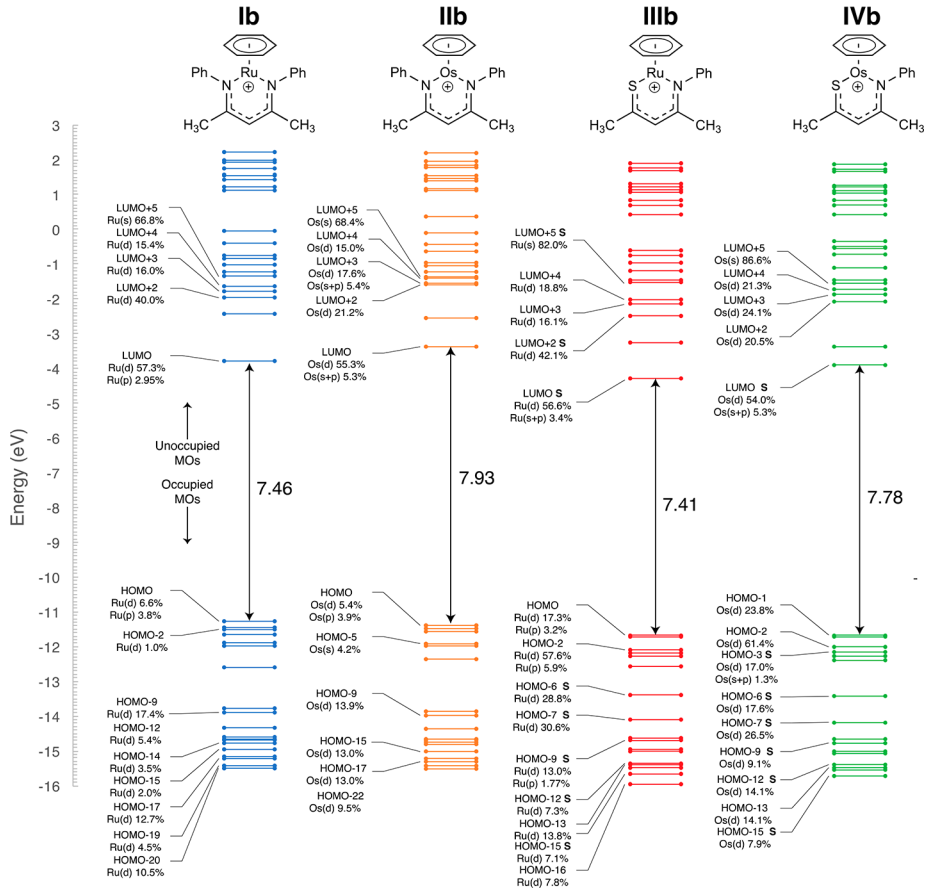

Figure 8. Comparison of the molecular orbital energy levels (DFT calculated, ωB97XD) for the highest occupied and lowest occupied MOs in the cationic Ru and Os complexes with β-diketiminate or β-thioketoiminate ligands (*N*-phenyl substituted). For those MOs which feature significant overlap between the metal and β-diketiminate/β-thioketoiminates are labelled. The contribution of metal d- and higher s- and p-orbitals are indicated as percentages. LUMOs and HOMOs with significant sulfur contribution are highlighted by the S label.

between different bond types.[68,69] The influence of sterics associated with the size of the *N*-aryl group are clearly evident, as the MBI shows stronger metal bonds for those species with the *N*-phenyl substituent (except for **IVa,b**), and the β-diketiminate complexes (**I** and **II**) demonstrating greater variance. Of note is the relatively high bond strength for the M−S bond in **III** and **IV** which is matched by weaker M−C(η^6-arene) and M−N bonds as compared to those in **I** and **II**. Furthermore, the Os−S bond in **IVa,b** is stronger than the corresponding Ru−S bond in **IIIa,b**, but conversely, the Ru−N bonds are stronger than those in **IVa,b**. As previously documented, the interaction between the η^6-arene and Os center is greater than that for Ru.[13] The increased bond order

DOI: 10.1021/acs.organomet.8b00111
Organometallics XXXX, XXX, XXX−XXX

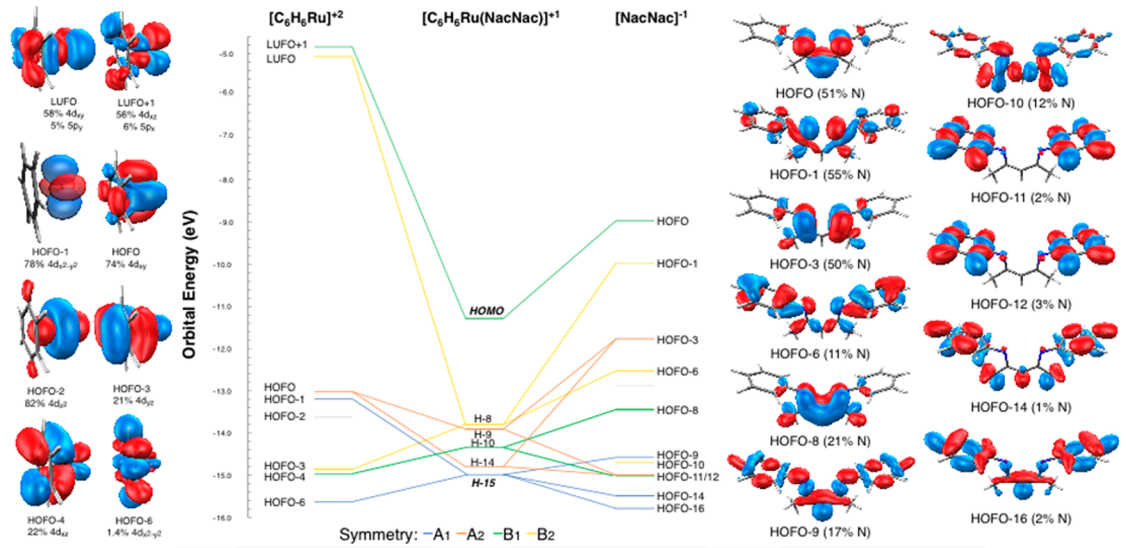

MO	[C6H6Ru]+2 FO	[NacNac]-1 FO	MO	[C6H6Ru]+2 FO	[NacNac]-1 FO	MO	[C6H6Ru]+2 FO	[NacNac]-1 FO
HOMO	LUFO+1 (14.6%)	HOFO (77.2%)	HOMO-9	HOFO (20.0%)	HOFO-3 (53.8%) HOFO-11 (19.6%)	HOMO-14	HOFO (4.5%)	HOFO-3 (12.7%) HOFO-11 (77.5%)
HOMO-8	LUFO (10.9%) HOFO-3 (25.6%)	HOFO-1 (13.2%) HOFO-6 (34.9%)	HOMO-10	HOFO-4 (4.1%)	HOFO-8 (44.1%) HOFO-12 (46.4%)	HOMO-15	HOFO-6 (3.3%) HOFO-1 (1.7%)	HOFO-9 (33.8%) HOFO-14(13.9%) HOFO-16(30.0%)

Figure 9. Orbital interaction diagram for the DFT (ωB97XD) energy optimized cationic η^6-C_6H_6 Ru *N*-phenyl-β-diketiminate optimized in C_{2v} symmetry. The MO−FO pairs are connected when each fragment (FO) contributes greater than 10% to the corresponding MO. The relative 5p and 4d orbital character for Ru and %N of the β-diketiminate ligand is given in parentheses.

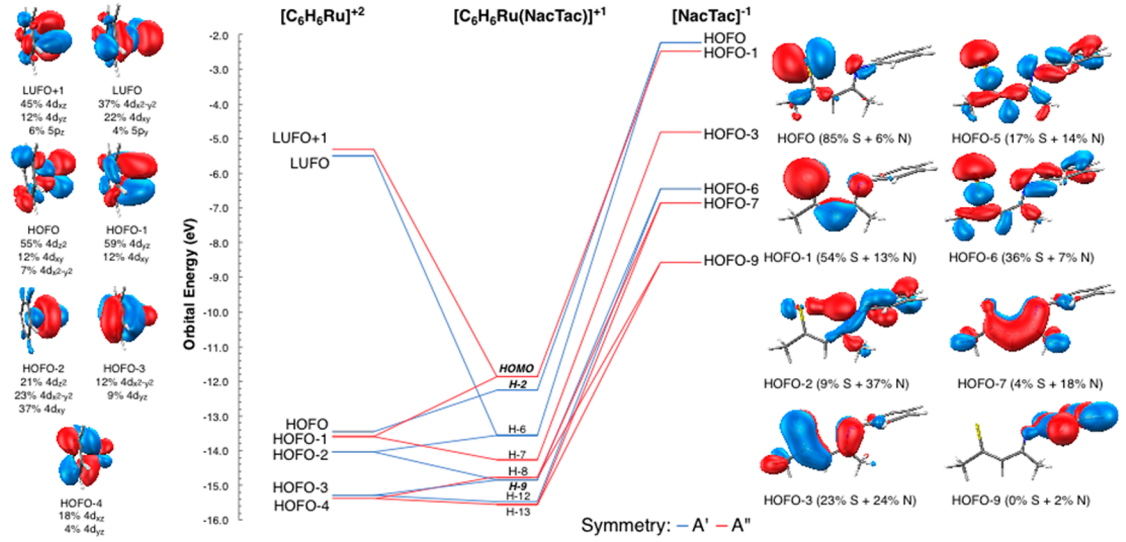

MO	[C6H6Ru]+2 FO	[NacTac]-1 FO	MO	[C6H6Ru]+2 FO	[NacTac]-1 FO	MO	[C6H6Ru]+2 FO	[NacTac]-1 FO	MO	[C6H6Ru]+2 FO	[NacTac]-1 FO
HOMO	LUFO+1 (12.2%) HOFO-1 (14.4%)	HOFO-1 (63.9%)	HOMO-6	LUFO (12.1%) HOFO-2 (28.1%)	HOFO (27.7%)	HOMO-8	HOFO-4 (4.3%)	HOFO-7 (51.6%) HOFO-9 (35.3%)	HOMO-12	HOFO-3 (13.8%)	HOFO-5 (23.9%) HOFO-6 (29.0%)
HOMO-2	HOFO (59.0%)	HOFO (13.3%)	HOMO-7	HOFO-1 (35.5%)	HOFO-3 (48.6)	HOMO-9	HOFO-2 (9.5%) HOFO-3 (8.1%)	HOFO-2 (17.8%) HOFO-5 (13.9%) HOFO-6 (14.5%)	HOMO-13	HOFO-4 (39.8%)	HOFO-7 (26.7%) HOFO-9 (22.8%)

Figure 10. Orbital interaction diagram for the DFT (ωB97XD) energy optimized cationic η^6-C_6H_6 Ru *N*-phenyl-β-thioketoiminate optimized in C_s symmetry. The MO-FO pairs are connected when each fragment (FO) contributes greater than 10% to the corresponding MO. The relative 5p and 4d orbital character for Ru and the %N and %S of the β-thioketoiminate ligand is given in parentheses.

about the metal center in **IVa,b** correlates with an increased in electron density at the Os center as compared to Ru in **IIIa,b**.

To probe further into the origins of the differences in electronic structure between the types of complexes, an examination of the energies of the frontier MOs was performed. For simplicity, only the less sterically hindered *N*-phenyl-substituted complexes (**Ia**−**IVa**) are considered herein. The energy levels of the highest occupied and lowest unoccupied MOs are shown in Figure 8. It is observed that the HOMOs of the β-diketiminate complexes (**Ia** and **IIa**) are split into two groupings, while a more even energy distribution of the HOMOs is present within the β-thioketoiminate complexes (**IIIa** and **IVa**). The corresponding HOMO−LUMO gaps are smaller in **IIIa** and **IVa**, which is caused mainly by the presence of lower energy LUMOs. Moreover, the contribution of metal d-orbital character is far more significant in the upper HOMOs for **IIIa** and **IVa**, while the LUMO character of all complexes is consistent in the amount of metal d-orbital character. Although some mixing of the higher 5s and 5p metal-based HOMOs and LUMOs is present, its contribution is relatively minor. Interestingly, the nitrogen contribution to metal bonding in **IIIa** and **IVa** is buried in the lower HOMOs.

DOI: 10.1021/acs.organomet.8b00111
Organometallics XXXX, XXX, XXX−XXX

Table 6. UV−Visible Data (λ_{max} and Molar Absorption (ε)) for Cationic η^6-C_6H_6 Ru and Os Complexes Supported by β-Thioketoiminate 7c and 8 and β-Diketiminate 2c and 2d Ligands[a]

7c (M = Ru)				**8** (M = Os)			
λ_{max} (nm)	ε (L mol^{-1} cm^{-1})	band	type	λ_{max} (nm)	ε (L mol^{-1} cm^{-1})	band	type
530	1875	A	$\pi \rightarrow$ d	507	1044	A	$\pi \rightarrow$ d
423	3075	B	$\pi \rightarrow$ d	432	1484	B	$\pi \rightarrow$ d
324	13077	C	$\pi \rightarrow \pi^*$	311	11440	C	$\pi \rightarrow \pi^*$
			d $\rightarrow$ d				d $\rightarrow$ d
279	20512	D	$\pi \rightarrow \pi^*$	279	13664	D	$\pi \rightarrow \pi$
264	28298	E	$\pi \rightarrow$ d	270	13868	E	$\pi \rightarrow$ d
2c (M = Ru)				**2d** (M = Os)			
λ_{max} (nm)	ε (L mol^{-1} cm^{-1})	band	type	λ_{max} (nm)	ε (L mol^{-1} cm^{-1})	band	type
437	7888	A	$\pi \rightarrow$ d	484	985		$\pi \rightarrow$ d
290	19039	B	d $\rightarrow \pi^*$	382	5149	A	$\pi \rightarrow$ d
			$\pi \rightarrow \pi^*$	302	19540	B	d $\rightarrow \pi^*$
			d $\rightarrow$ d				$\pi \rightarrow \pi^*$
							d $\rightarrow$ d

[a]Recorded in anhydrous CH_2Cl_2.

To quantify even further the metal bonding differences, charge decomposition analyses (CDA) were performed using the procedure developed by Frenking et al.[70−72] Two separate CDA analyses were performed, one involving the anionic ligand and $[\eta^6$-$C_6H_6M]^{2+}$ (M = Ru and Os) fragments and the second between the neutral η^6-arene and the negatively charged metal β-diketiminate or β-thioketoiminate fragments. Table S7 indicates the amount of forward and back electron donation between the fragments, which can be further subdivided into individual symmetric components related to σ- and π-type bonding.

The CDA reveals that the β-diketiminate ligand is both a strong σ and moderate π e^- donor with almost a negligible amount of σ- or π-back-donation from the metal. In contrast, the β-thioketoiminate ligand is not only a strong σ- and moderate π-donor, but also receives more electron density back from the η^6-arene metal fragment due to the better electron accepting properties of sulfur. This correlates well with the calculated high strength for the metal−sulfur bonds from the MBI values which fully justifies the strong thiophilicity observed for Ru and Os.[73] An examination of the second CDA (Table S8) between the η^6-arene and metal β-diketiminate/β-thioketoiminate fragments reveals greater forward charge transfer (CT) from the ligand to metal, which in the case of the β-diketiminate species (**Ia** and **IIa**) is matched by strong backward CT from the metal. For β-thioketoiminates (**IIIa** and **IVa**), the absolute amount of forward and backward CT are reduced, but the forward/backward (f/b) ratio is consistent with **Ia** and **IIa**. Both types of Os complexes (**IIa** and **IVa**) demonstrate a greater tendency to participate in back-bonding with the arene. The CDA affords the possibility to identify the upper HOMOs that contribute to bonding between the metal and chelating ligands. Figures 9 and 10 show the results for both types of cationic Ru complexes, **Ia** and **IIIa**. The figures highlight those interactions where orbital overlap between (fragment orbitals) FOs is maximized. However, not all overlap interactions result in significant forward or backward charge transfer between the fragments. In the case of **Ia**, the HOFOs (highest occupied fragment orbitals) of the β-diketiminate are divided between in-phase and out-of-phase σ- and π-type MOs as previously documented.[7] HOFO and HOFO-2 of the β-diketiminate combine exclusively with the LUFOs of the arene−Ru fragment (Ru $4d_{xy}$ and $4d_{xz}$) resulting in HOMO and HOMO−8 which account for the greatest amount of forward CT. The HOMO is a B_1 π-type interaction is composed of an allylic N−Ru−N arrangement which strongly stabilizes this class of cationic 16e$^-$ complex. Other π-type interactions arise from the combination of β-diketiminate HOFO-3 and HOFO-8 with the $4d_{xz}$ of Ru resulting in a moderate degree of stabilizing CT. In general, the A_1 out-of-phase σ-type interactions are the most dominant and form occupied MOs within **Ia** at lower energies. The in-phase HOFO-2 of the chelating ligand forms a weak overlap with the only phase compatible Ru $4d_z^2$ orbital. Bonding interactions with greater η^6-arene-metal contribution are associated with lower HOMOs, i.e., HOMO−15 and HOMO−19.

In the case of **IIIa**, the FO interaction diagram (Figure 10) is more complicated owing to the lower molecular symmetry C_s, where the FOs of the η^6-C_6H_6Ru fragment are of mixed d-orbital character; however, the sum of the d-orbital contribution **IIIa** remains constant in comparison to that of **Ia**. One striking difference between the different types of complexes are the relative energies of the HOFO and LUFO associated with the η^6-arene-Ru fragment. In **Ia**, from the f/b CT values shown in Table S7, the greater forward CT in the β-diketiminate case serves to increase the over orbital energies of the arene−Ru fragment (HOFO −13.02 eV, LUFO −5.07 eV) and prevent these HOFOs from effectively mixing with the upper HOFOs of the β-diketiminate. Instead, for **IIIa** the lower energies of the LUFOs associated with the arene−Ru fragment (HOFO −13.32 eV, LUFO −5.37 eV) results in a combined contribution of LUFOs and HOFOs with the upper S-based HOFOs of the β-thioketoiminate ligand. It is clear that the β-thioketoiminate HOFOs with dominant sulfur character (HOFO and HOFO−1) are positioned at higher energy and combine to a greater extent with occupied and unoccupied FOs of the η^6-arene−Ru fragment, forming lower energy HOMOs. Thus, the HOFOs with dominant N character form weaker overlaps with the arene-Ru fragment, thus correlating with reduced Ru−N bond strength.

In contrast to **Ia**, for **IIIa** additional FO interactions result in forward ligand to metal CT distributed amid the HOMOs of the complex. The largest CT being associated with HOMO−2 (σ-type), HOMO (π-type) and HOMO−6 (σ-type) with the

DOI: 10.1021/acs.organomet.8b00111
Organometallics XXXX, XXX, XXX−XXX

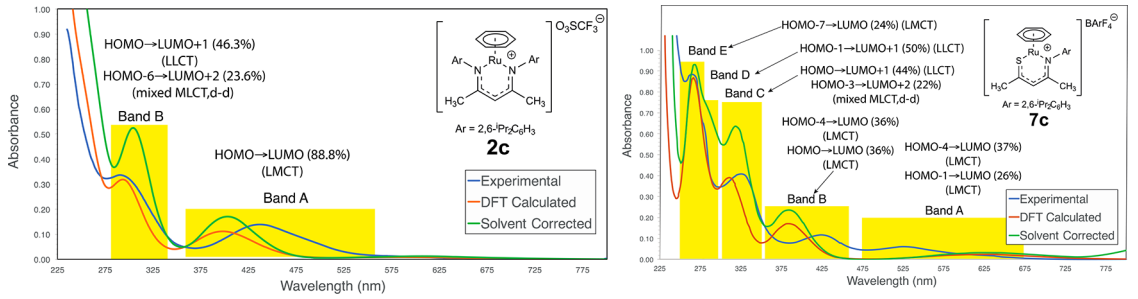

Figure 11. Comparison of experimental (CH_2Cl_2), TD-DFT (ωB97XD, gas phase) and TD-DFT (ωB97XD, CPCM-CH_2Cl_2 corrected) optical absorption spectra for cationic η^6-C_6H_6 Ru *N*-2,6-diisopropylphenyl-β-diketiminate (top) η^6-C_6H_6 Ru *N*-2,6-diisopropylphenyl-β-thioketoiminate (bottom). The contribution of each type of transition to overall absorption is given in parentheses.

FOs of the β-thioketoiminate with dominant S character contributing mainly to the CT. Interestingly, the out-of-phase HOFO-2 of the chelating ligand shows reduced metal to ligand MO overlap but is one of the main sources of metal to ligand backward CT. As indicated by the CDA, back e^- donation from the Ru to S originates in HOMO−5 (σ-type) and HOMO−7 (π-type), where the latter is composed of a bonding interaction between HOFO−1 and $4d_{yz}$ of Ru.

Overall, the metal−ligand bonding in **1a** is dominated by an allylic-type N−Ru−N interaction which involves significant σ-based and π-based CT from the N centers to the Ru; in turn, this excess e^- density is transferred to the η^6-arene. In contrast, for **IIIa**, β-thioketoiminate to metal CT is not as significant but a more efficient MO overlap (greater covalency) between the metal and S which enables backward CT; hence, the metal ligand bonding in **IIIa** is dominated by the metal−sulfur interaction. Thus, both types of complexes featuring both low coordinate cationic metal centers are significantly stabilized, but by different internal bonding mechanisms. The presence of a nucleophilic β-C site suggests that both types of complex demonstrate similar types of reactivity, specifically a strong preference to undergo [4 + 2] cycloadditions with π-bonded substrates over direct metal coordination with purely σ-donating molecules.

Electronic Absorption. For the cationic complexes bearing the 2,6-^{i}Pr$_2$C$_6$H$_3$ substituent, **2c**, and **7c**,**8**, the UV−visible adsorption spectra were recorded in CH_2Cl_2. λ_{maxima} and the associated molar absorptivity values are given in Table 6. The experimentally obtained spectra for the two types of Ru species are shown in Figure 11, whereas the corresponding Os species are given in Figures S10 and S11. Each type of complex presents with same number of absorptions regardless of the metal type, with exception that Os species **2d** has an additional low energy adsorption. Using time-dependent DFT (TD-DFT) techniques, the first 80 excitations were modeled with solvent corrections,[74] and the resulting simulated spectra were shown in good agreement with experimental data. The lower energy transitions (band A) of the TD-DFT predictions were blue-shifted as compared to the experimental data. The magnitude of the differences in predicted λ_{maxima} are routinely observed in other type of Ru complexes.[72,75] Each absorption band was matched with electronic transitions between specific MOs; see the Supporting Information for a graphical description of the upper HOMOs and LUMOs for each type of Ru complex. The higher symmetric Ru β-diketiminate complex, **2c** (C_{2v}), presents with a simplified spectrum dominated by two absorption bands. The first absorption corresponds to a symmetry allowed HOMO (b_1) to LUMO (b_1) transition of LMCT type. The second absorption is an uneven mixture between a symmetry-disallowed LLCT of HOMO+1 to LUMO +1 and MLCT of HOMO−6 to LUMO+2. Interestingly, HOMO−6 is a source of significant forward CT from the β-diketiminate ligand to the η^6-arene-Ru fragment. The rest of the higher energy absorptions are merged and unresolved due to limits of solvent adsorption. In contrast, the Ru β-thioketoiminate species **7c** has five distinct absorption bands, with the first band (A) occurring at higher wavelengths, comprising two LMCTs, where the receiving LUMO has dominant S-based character, contributing to the lower energy of this MO. Band B is composed of another two LMCTs corresponding to band A in the Ru β-diketiminate complex and features strong S character in both the HOMO and LUMO. Similarly, band C, mainly a LLCT between the HOMO and LUMO+1, also features a minor contribution from a MLCT and d−d transition. This band is equivalent to band B in the β-diketiminate species. Band D, observed in the experimental spectra, was only resolved in the solvent-corrected TDDFT calculated spectra and corresponds to another LLCT. Finally, absorption E is a high-energy LMCT from the lower energy HOMO−7 to the LUMO and is equivalent to band B in **2c**. This band features an π-type orbital overlap between the Ru, S, and N centers and is associated with a strong CT from the chelating ligand to the metal center. Os β-diketiminate complex **2d** differs mainly from the Ru analogue in that band A shows a hypsochromic shift, while band B is bathochromic shifted, where the MLCT and LLCT become more separated. The situation in the case of the Os β-thioketoiminate species **8**, is more complicated where bands B−D have merged, and band E is hypsochromic shifted into the solvent cutoff region.

CONCLUSIONS

Conversion of the β-ketoiminates to the corresponding β-thioketoiminates or β-selenoketoiminates was made possible by reacting with the appropriate chalcogen transfer reagent. Deprotonation of β-thioketoiminates with *n*-BuLi enables transmetalation and N,S-bidentate coordination to an η^6-C_6H_6 Ru(II) or Os(II) moiety. In contrast, the β-selenoketoiminates were found to be too unstable to complete the coordination process. Cationic 16-electron Ru(II) and Os(II) complexes supported by the β-thioketoiminate ligand were facilitated by employing an appropriate Cl abstraction reagent. Diagnostic NMR resonances, i.e., β-H and protons of the η^6-C_6H_6 group indicate that the β-thioketoiminate ligand strongly interacts with the metal center. The experimental observations are fully supported by the MBI values and CDA from DFT calculations, which indicates that M−S interaction

DOI: 10.1021/acs.organomet.8b00111
Organometallics XXXX, XXX, XXX−XXX

within the cationic containing β-thioketoiminates species is dominant due to favorable forward and backward π- and σ-type donations resulting from effective MO overlap between the thio-carbonyl group and metal center. The reactivity of the cationic η^6-arene Ru β-thioketoiminate complex generally parallels that of the β-diketiminate analogues in that combination with alkynes results in cycloaddition products and coordination with π-accepting aryl-isonitriles afforded octahedral Ru(II) complexes with two equatorial *trans*-positioned isonitriles and two axial isonitrile ligands. Attempts to engage the formal lone pair on the S center on the cationic η^6-arene Ru β-thioketoiminates with Lewis acids were not successful. The herein newly reported complexes are being further investigated in potential catalytic applications.

EXPERIMENTAL SECTION

General Procedures. The synthesis of the precursory ligands, reagents, and final complexes was carried out under a purified inert atmosphere of N_2 using standard Schlenk techniques. Manipulations of all products and reagents, including preparation of samples for NMR analysis were performed in an Innovative Technologies glovebox with a N_2 atmosphere containing less than 1 ppm of O_2 and H_2O.[76,77] All glassware was predried, and the flasks underwent several purge/refill cycles before the introduction of solvents or reagents. All solvents were dried according to literature procedures involving distillation over the appropriate drying agents[78] and stored in Schlenk flasks equipped with a Teflon stopcock. Celite for filtration was kept in an oven at 130 °C and degassed prior to use. All other reagents and gases (technical-grade) were purchased from commercial sources and used as received if not otherwise specified. The syntheses of the bis(dichloro(η^6-benzene)ruthenium(II)) and bis(dichloro(η^6-benzene)osmium(II)) dimers were carried out by a slightly modified procedure according to Bennett et al. and Stephenson et al., respectively.[58,79] Anhydrous sodium tetrakis(3,5-bis(trifluoromethylphenyl)borate $[Na]BAr^F_4$, (BAr^F_4 = $B(3,5\text{-}(CF_3)_2C_6H_3)_4$) was synthesized according to procedures outlined by Reger et al.[80] The precursory β-ketoiminate ligands were synthesized according the method published by Cowley et al.[81] η^6-Arene Ru and Os β-diketiminate complexes **2c,d** were prepared as previously described by Phillips et al.[12,13] Synthesis and characterization of complexes **2b−d** and **9−13**, details including instrumentation used for structural characterization, and specifics regarding the DFT calculations are available in the Supporting Information.

General Procedure for β-Thioketoimines Synthesis. Ligands **3a−d** were prepared using a modified method similar to that described by Walter et al.[29] The starting β-ketoiminate (1 equiv, 10 mmol) was dissolved in dry 1,2-dimethoxyethane (40 mL) at room temperature. Commercially purchased Lawesson's reagent (0.5 equiv, 5 mmol) was added to give a yellow solution. The reaction was stirred overnight under N_2 to give a dark red solution. The solution was then added to distilled water (100 mL) affording a yellow-orange biphasic mixture. Dichloromethane (50 mL) and saturated brine (20 mL) were added, and the resulting mixture was stirred for 30 min. The organic layer was separated, and the aqueous layer was extracted with dichloromethane (50 mL). The organic layers were combined and dried over anhydrous sodium sulfate. The solvent was removed under reduced pressure, and the resulting red oil was purified by passage through a plug of silica gel/alumina (basic) 1:1, using dichloromethane as the eluent. All volatiles were removed under reduced pressure to leave the product as a red oil which solidified upon standing.

General Synthesis of β-Aminoselenones. The desired β-ketoiminate (1 equiv, 3.6 mmol) was dissolved in dry toluene (40 mL) at room temperature. Commercially purchased Woollins' reagent (0.5 equiv, 1.8 mmol) was added to instantly afford a deep colored red solution. The reaction was stirred overnight under an N_2 atmosphere to give a dark red solution, whereby another 0.5 equiv Woollins' reagent was added. The reaction was then stirred for a total of 1 week. The resulting red solution was purified by passing through a plug of silica gel/alumina (basic) 1:1, using dichloromethane as eluent. The solvent was removed under reduced pressure affording the product as a red viscous oil.

General Synthesis of Chloro−Arene Ru(II) or Os(II)-β-Thioketoiminate Complexes. The selected *in situ* generated Li-β-thioketoiminate (1 equiv, 1.8 mmol) and 0.5 equiv of either the Ru(II) or Os(II) dimeric precursor (i.e., $(M(\eta^6\text{-}C_6H_6)Cl_2)_2$ M = Ru or Os) were dissolved in dry dichloromethane (10 mL). After stirring overnight under a N_2 atmosphere, the dark colored red solution was filtered through 1 cm of Celite and the solvent removed under reduced pressure to a total volume of approximately 1 mL. Dry *n*-pentane (10 mL) was added to precipitate the product as a powder, which was dried under reduced pressure for 4 to 12 h.

General Synthesis. *Method A (Chlorido Abstraction).* A single equivalent of the selected chlorido-Ru(II)- or -Os(II)-thioketoiminate complex (1 mmol) and the required chloride abstraction agent, i.e., $[Ag]PF_6$, $[Ag]SbF_6$ or $[Na]B(C_6H_3(m\text{-}CF_3)_2)_4$ (1.2 equiv, 1.2 mmol) were dissolved together in dry dichloromethane (10 mL). When silver salts were employed, the reaction vessel was protected from light. After stirring overnight under an N_2 inert atmosphere, the resulting dark green solution was filtered through Celite and the volume of the solvent adjusted to a volume of approximately 1 mL under reduced pressure. Dry *n*-pentane (10 mL) was added to precipitate the product as a powder which was dried for 4−12 h under reduced pressure.

Method B (Direct Synthesis of Salts Containing the Cationic (η^6-C_6H_6) Ru(II) or Os(II) β-Thioketoiminate). The selected Li-β-thioketoiminate (1 equiv, 1.8 mmol), combined with the Ru(II) dimeric precursor $(Ru(\eta^6\text{-}C_6H_6)Cl_2)_2$ (0.5 equiv, 0.9 mmol) and $[Na]SO_3CF_3$ (1.2 equiv, 2.2 mmol), was dissolved in dry dichloromethane (10 mL). After stirring overnight under a N_2 atmosphere, the dark brown solution was filtered through Celite, and the volume of solvent was adjusted to approximately 1 mL under reduced pressure. Dry *n*-pentane (10 mL) was added to precipitate the product as a powder which was dried for 4−12 h under reduced pressure.

ASSOCIATED CONTENT

Supporting Information

The Supporting Information is available free of charge on the ACS Publications website at DOI: 10.1021/acs.organomet.8b00111.

Additional instrumentation details and synthesis and characterization of all ligands and complexes; supplementary solid-state structural details for complexes **5b**, **6**, **8**, **13**, **2c−d**; additional computational details including geometry and charge comparisons, selected MO diagrams, and experimental/TDDFT-predicted optical spectra for **8** and **2d** (PDF)

Atomic coordinates of all optimized structures (XYZ)

Accession Codes

CCDC 1825143−1825152 contain the supplementary crystallographic data for this paper. These data can be obtained free of charge via www.ccdc.cam.ac.uk/data_request/cif, or by emailing data_request@ccdc.cam.ac.uk, or by contacting The Cambridge Crystallographic Data Centre, 12 Union Road, Cambridge CB2 1EZ, UK; fax: +44 1223 336033.

AUTHOR INFORMATION

Corresponding Author

*E-mail: andrew.phillips@ucd.ie.

ORCID

Andrew D. Phillips: 0000-0001-5599-6499

Notes

The authors declare no competing financial interest.

DOI: 10.1021/acs.organomet.8b00111
Organometallics XXXX, XXX, XXX−XXX

■ ACKNOWLEDGMENTS

This work was also supported through Science Foundation Ireland (SFI) for the Solar Energy Conversion Cluster under Grant [07/SRC/B1160]. Additionally, A.D.P. thanks Science Foundation Ireland (SFI) for a Stokes Lectureship held at the school of chemistry, UCD. We are grateful for the access to computing facilities owned and operated by the Irish Centre for High-End Computing (ICHEC).

■ REFERENCES

(1) Webster, R. L. *Dalton Trans.* **2017**, *46*, 4483−4498.
(2) Camp, C.; Arnold, J. *Dalton Trans.* **2016**, *45*, 14462−14498.
(3) Chen, C.; Bellows, S. M.; Holland, P. L. *Dalton Trans.* **2015**, *44*, 16654−16670.
(4) Phillips, A. D. *Organometallic Chemistry* **2014**, *39*, 72−147.
(5) Zhu, D.; Budzelaar, P. H. M. *Dalton Trans.* **2013**, *42*, 11343−11354.
(6) Tsai, Y.-C. *Coord. Chem. Rev.* **2012**, *256*, 722−758.
(7) Bourget-Merle, L.; Lappert, M. F.; Severn, J. R. *Chem. Rev.* **2002**, *102*, 3031−3066.
(8) Holland, P. L. *Acc. Chem. Res.* **2008**, *41*, 905−914.
(9) Smith, J. M.; Lachicotte, R. J.; Pittard, K. A.; Cundari, T. R.; Lukat-Rodgers, G.; Rodgers, K. R.; Holland, P. L. *J. Am. Chem. Soc.* **2001**, *123*, 9222−9223.
(10) Monillas, W. H.; Young, J. F.; Yap, G. P. A.; Theopold, K. H. *Dalton Trans.* **2013**, *42*, 9198−9210.
(11) Moreno, A.; Pregosin, P. S.; Laurenczy, G.; Phillips, A. D.; Dyson, P. J. *Organometallics* **2009**, *28*, 6432−6441.
(12) Phillips, A. D.; Laurenczy, G.; Scopelliti, R.; Dyson, P. J. *Organometallics* **2007**, *26*, 1120−1122.
(13) Schreiber, D. F.; O'Connor, C.; Grave, C.; Müller-Bunz, H.; Scopelliti, R.; Dyson, P. J.; Phillips, A. D. *Organometallics* **2013**, *32*, 7345−7356.
(14) Phillips, A. D.; Zava, O.; Scopelitti, R.; Nazarov, A. A.; Dyson, P. J. *Organometallics* **2010**, *29*, 417−427.
(15) Schreiber, D. F.; Ortin, Y.; Müller-Bunz, H.; Phillips, A. D. *Organometallics* **2011**, *30*, 5381−5395.
(16) Grützmacher, H. *Angew. Chem., Int. Ed.* **2008**, *47*, 1814−1818.
(17) Khusnutdinova, J. R.; Milstein, D. *Angew. Chem., Int. Ed.* **2015**, *54*, 12236−12273.
(18) Schreiber, D. F.; O'Connor, C.; Grave, C.; Ortin, Y.; Müller-Bunz, H.; Phillips, A. D. *ACS Catal.* **2012**, *2*, 2505−2511.
(19) Mori, S.; Mochida, T. *Organometallics* **2013**, *32*, 780−787.
(20) Shin, R. Y. C.; Bennett, M. A.; Goh, L. Y.; Chen, W.; Hockless, D. C. R.; Leong, W. K.; Mashima, K.; Willis, A. C. *Inorg. Chem.* **2003**, *42*, 96−106.
(21) Yamamoto, Y.; Sakamoto, S.; Ohki, Y.; Usuzawa, A.; Fujita, M.; Mochida, T. *Dalton Trans.* **2003**, 3534−3540.
(22) Sharma, A. K.; Joshi, H.; Sharma, K. N.; Gupta, P. L.; Singh, A. K. *Organometallics* **2014**, *33*, 3629−3639.
(23) Levason, W.; Ollivere, L. P.; Reid, G.; Webster, M. *J. Organomet. Chem.* **2010**, *695*, 1346−1352.
(24) Kumar P., R.; Singh, A. K.; Butcher, R. J.; Sharma, P.; Toscano, R. A. *Eur. J. Inorg. Chem.* **2004**, *2004*, 1107−1114.
(25) Singh, P.; Singh, A. K. *Organometallics* **2010**, *29*, 6433−6442.
(26) Duguay, G.; Metayer, C.; Quiniou, H. *Bull. Soc. Chim. Fr.* **1974**, *11*, 2507−12.
(27) Ozturk, T.; Ertas, E.; Mert, O. *Chem. Rev.* **2007**, *107*, 5210−5278.
(28) Jesberger, M.; Davis, T. P.; Barner, L. *Synthesis* **2003**, *13*, 1929−1958.
(29) Walter, W.; Proll, T. *Synthesis* **1979**, *1979*, 941−942.
(30) Solov'ev, A. V.; Chernega, A. N.; van Almsick, A.; Hoffmann, M. G.; Shermolovich, Y. G. Z. *Z. Anorg. Allg. Chem.* **2005**, *631*, 2842−2847. Bansse, W.; Uhlemann, E.; Weller, F. *Z. Kristallogr. - Cryst. Mater.* **1996**, *211*, 955−956.
(31) Beardwood, P.; Gibson, J. F. *J. Chem. Soc., Chem. Commun.* **1983**, 1099−1101.
(32) Yadav, D. D. S.; Mehrotra, R. C. *Inorg. Chim. Acta* **1985**, *96*, 39−42.
(33) Kraudelt, H.; Schilde, U.; Uhlemann, E. *Z. Kristallogr. - New Cryst. Struct.* **1998**, *213*, 175.
(34) Ruiz Plaza, D.; Alvarado-Monzón, J. C.; Andreu de Riquer, G. A.; González-García, G.; Höpfl, H.; de León-Rodríguez, L. M.; López, J. A. *Eur. J. Inorg. Chem.* **2016**, *2016*, 874−879.
(35) Zharkova, G. I.; Baidina, I. A. *Russ. J. Coord. Chem.* **2009**, *35*, 36−41.
(36) Nivorozhkin, L. E.; Olekhnovich, R. Y.; Korobov, M. S.; Konstantinokii, L. E.; Minkin, V. I. *Koord. Khim.* **1986**, *12*, 899−906.
(37) Kingsbury, J. S.; Harrity, J. P. A.; Bonitatebus, P. J.; Hoveyda, A. H. *J. Am. Chem. Soc.* **1999**, *121*, 791−799.
(38) Hoskins, B. F.; Robson, R.; Williams, G. A.; Wilson, J. C. *Inorg. Chem.* **1991**, *30*, 4160−4166.
(39) Hoskins, B. F.; McKenzie, C. J.; Robson, R.; Zhenrong, L. *J. Chem. Soc., Dalton Trans.* **1990**, 2637−2641.
(40) Marin-Becerra, A.; Stenson, P. A.; McMaster, J.; Blake, A. J.; Wilson, C.; Schröder, M. *Eur. J. Inorg. Chem.* **2003**, *2003*, 2389−2392.
(41) Mugesh, G.; Singh, H. B.; Butcher, R. J. *Eur. J. Inorg. Chem.* **1999**, *1999*, 1229−1236.
(42) Goswami, N.; Eichhorn, D. M. *Inorg. Chem.* **1999**, *38*, 4329−4333.
(43) Marini, P. J.; Berry, K. J.; Murray, K. S.; West, B. O.; Irving, M.; Clark, P. E. *J. Chem. Soc., Dalton Trans.* **1983**, 879−884.
(44) Hua, G.; Woollins, J. D. *Angew. Chem., Int. Ed.* **2009**, *48*, 1368−1377.
(45) Hua, G.; Li, Y.; Slawin, A. M. Z.; Woollins, J. D. *Org. Lett.* **2006**, *8*, 5251−5254.
(46) Gray, I. P.; Bhattacharyya, P.; Slawin, A. M. Z.; Woollins, J. D. *Chem. - Eur. J.* **2005**, *11*, 6221−6227.
(47) Brownstein, S.; Gabe, E. J.; Prasad, L. *Can. J. Chem.* **1983**, *61*, 1410−1413.
(48) Stender, M.; Wright, R. J.; Eichler, B. E.; Prust, J.; Olmstead, M. M.; Roesky, H. W.; Power, P. P. *Dalton Trans.* **2001**, 3465−3469.
(49) Gietz, T.; Boeré, R. T. *Inorganics* **2017**, *5*, 30.
(50) Kalinowski, H.-O.; Berger, S.; Braun, S. *Carbon-13 NMR Spectroscopy*. John Wiley and Sons: New York, 1988.
(51) Andrieu, C. G.; Debruyne, D.; Paquer, D. *Org. Magn. Reson.* **1978**, *11*, 528−532.
(52) Schneider, M.; Gil, M. J.; Reliquet, A.; Meslin, J. C.; Levillain, J.; Vazeux, M.; Jury, D.; Mieloszynski, J. L.; Paquer, D. *Phosphorus, Sulfur Silicon Relat. Elem.* **1998**, *134*, 295−305.
(53) Surya Prakash, G. K.; Mathew, T. Sodium 1,1,1-Trifluoromethanesulfonate. In *Encyclopedia of Reagents for Organic Synthesis*; John Wiley & Sons, Ltd, 2001.
(54) Fulmer, G. R.; Miller, A. J. M.; Sherden, N. H.; Gottlieb, H. E.; Nudelman, A.; Stoltz, B. M.; Bercaw, J. E.; Goldberg, K. I. *Organometallics* **2010**, *29*, 2176−2179.
(55) Kalinowski, H.-O.; Kessler, H. *Angew. Chem., Int. Ed. Engl.* **1974**, *13*, 90−91.
(56) Balci, M. Chapter 12 - Chemical Shift. In *Basic ^{1}H- and ^{13}C-NMR Spectroscopy*; Elsevier Science: Amsterdam, 2005; pp 283−292.
(57) Groom, C. R.; Bruno, I. J.; Lightfoot, M. P.; Ward, S. C. *Acta Crystallogr., Sect. B: Struct. Sci., Cryst. Eng. Mater.* **2016**, *72*, 171−9.
(58) Bennett, M. A.; Smith, A. K. *J. Chem. Soc., Dalton Trans.* **1974**, 233−241.
(59) Yamamoto, Y.; Tanase, T.; Sudoh, C.; Turuta, T. *J. Organomet. Chem.* **1998**, *569*, 29−37.
(60) Cadierno, V.; Díez, J.; García-Álvarez, J.; Gimeno, J. *Organometallics* **2008**, *27*, 1809−1822.
(61) Walsh, A. P.; Brennessel, W. W.; Jones, W. D. *Inorg. Chim. Acta* **2013**, *407*, 131−138.
(62) Shin, R. Y. C.; Tan, G. K.; Koh, L. L.; Vittal, J. J.; Goh, L. Y.; Webster, R. D. *Organometallics* **2005**, *24*, 539−551.
(63) Frisch, M. J.; Trucks, G. W.; Schlegel, H. B.; Scuseria, G. E.; Robb, M. A.; Cheeseman, J. R.; Scalmani, G.; Barone, V.; Mennucci, B.; Petersson, G. A.; Nakatsuji, H.; Caricato, M.; Li, X.; Hratchian, H. P.; Izmaylov, A. F.; Bloino, J.; Zheng, G.; Sonnenberg, J. L.; Hada, M.;

DOI: 10.1021/acs.organomet.8b00111
Organometallics XXXX, XXX, XXX−XXX

Ehara, M.; Toyota, K.; Fukuda, R.; Hasegawa, J.; Ishida, M.; Nakajima, T.; Honda, Y.; Kitao, O.; Nakai, H.; Vreven, T.; Montgomery, J. A., Jr.; Peralta, J. E.; Ogliaro, F.; Bearpark, M.; Heyd, J. J.; Brothers, E.; Kudin, K. N.; Staroverov, V. N.; Kobayashi, R.; Normand, J.; Raghavachari, K.; Rendell, A.; Burant, J. C.; Iyengar, S. S.; Tomasi, J.; Cossi, M.; Rega, N.; Millam, J. M.; Klene, M.; Knox, J. E.; Cross, J. B.; Bakken, V.; Adamo, C.; Jaramillo, J.; Gomperts, R.; Stratmann, R. E.; Yazyev, O.; Austin, A. J.; Cammi, R.; Pomelli, C.; Ochterski, J. W.; Martin, R. L.; Morokuma, K.; Zakrzewski, V. G.; Voth, G. A.; Salvador, P.; Dannenberg, J. J.; Dapprich, S.; Daniels, A. D.; Farkas, O.; Foresman, J. B.; Ortiz, J. V.; Cioslowski, J.; Fox, D. J. *Gaussian 09*, revision E.01; Gaussian, Inc.: Wallingford, CT, 2009.

(64) Chai, J.-D.; Head-Gordon, M. *J. Chem. Phys.* **2009**, *131*, 174105.

(65) Harvey, J. N. *Annu. Rep. Prog. Chem., Sect. C: Phys. Chem.* **2006**, *102*, 203−226.

(66) Hirshfeld, F. L. *Theor. Chim. Acta* **1977**, *44*, 129−138.

(67) Marenich, A. V.; Jerome, S. V.; Cramer, C. J.; Truhlar, D. G. *J. Chem. Theory Comput.* **2012**, *8*, 527−541.

(68) Bridgeman, A. J.; Cavigliasso, G.; Ireland, L. R.; Rothery, J. *Dalton Trans.* **2001**, 2095−2108.

(69) Mayer, I. *J. Comput. Chem.* **2007**, *28*, 204−221.

(70) Dapprich, S.; Frenking, G. *J. Phys. Chem.* **1995**, *99*, 9352−9362.

(71) Frenking, G.; Matthias Bickelhaupt, F. The EDA Perspective of Chemical Bonding. In *The Chemical Bond*; Wiley-VCH Verlag; pp 121−157.

(72) Gorelsky, S. I.; Lever, A. B. P. *J. Organomet. Chem.* **2001**, *635*, 187−196.

(73) Kepp, K. P. *Inorg. Chem.* **2016**, *55*, 9461−9470.

(74) Skyner, R. E.; McDonagh, J. L.; Groom, C. R.; van Mourik, T.; Mitchell, J. B. O. *Phys. Chem. Chem. Phys.* **2015**, *17*, 6174−6191.

(75) Barolo, C.; Nazeeruddin, M. K.; Fantacci, S.; Di Censo, D.; Comte, P.; Liska, P.; Viscardi, G.; Quagliotto, P.; De Angelis, F.; Ito, S.; Grätzel, M. *Inorg. Chem.* **2006**, *45*, 4642−4653.

(76) Komiya, S. *Synthesis of Organometallic Compounds: A Practical Guide*; Wiley: Chichester, 1997.

(77) Shriver, D. F.; Drezdzon, M. A. *The Manipulation of Air-Sensitive Compounds*, 2nd ed.; Wiley: Chichester, 1986.

(78) Armarego, W. L. F.; Chai, C. *Purification of Laboratory Chemicals*, 7th ed.; Butterworth-Heinemann: Boston, 2013.

(79) Arthur, T.; Stephenson, T. A. *J. Organomet. Chem.* **1981**, *208*, 369−387.

(80) Lesley, M. J. G.; Norman, N. C.; Rice, C. R.; Reger, D. L.; Little, C. A.; Lamba, J. J. S.; Brown, K. J.; Peters, J. C.; Thomas, J. C.; Sahasrabudhe, S.; Yearwood, B. C.; Atwood, D. A.; Hill, R. F.; Wood, G. L.; Danzer, R.; Paine, R. T.; Wagner, N. L.; Murphy, K. L.; Haworth, D. T.; Bennett, D. W.; Byers, P. K.; Canty, A. J.; Honeyman, R. T.; Arnáiz, F. J.; Miranda, M. J.; Bohle, D. S.; Sagan, E. S.; Chivers, T.; Sandblom, N.; Schatte, G. *Inorg. Synth.* **2004**, 1−48.

(81) Gordon, J. C.; Shukla, P.; Cowley, A. H.; Jones, J. N.; Keogh, D. W.; Scott, B. L. *Chem. Commun.* **2002**, 2710−2711.

DOI: 10.1021/acs.organomet.8b00111
Organometallics XXXX, XXX, XXX−XXX